

**Development and Evaluation of Assessment and Management Strategies for
Pacific Salmon Fisheries in Western Alaska**

by

Benjamin A. Staton

A Dissertation submitted to the Graduate Faculty of
Auburn University
in partial fulfillment of the
requirements for the Degree of
Doctor of Philosophy

Auburn, Alabama
May 4, 2019

Keywords: Pacific salmon, phenological forecasts, management strategy evaluation,
mixed-stock fisheries, Bayesian inference

Copyright 2019 by Benjamin A. Staton

Approved by

Matthew J. Catalano, Chair, Professor of Fisheries, Aquaculture, and Aquatic Sciences
Asheber Abebe, Professor of Mathematics and Statistics

Lewis G. Coggins, Jr., Affiliate Professor of Fisheries, Aquaculture, and Aquatic Sciences
Conor P. McGowan, Professor of Wildlife and Forestry Sciences

Abstract

I'm going to write an abstract to go here. This paragraph will be a brief introduction chapter 1: the overall topic of the research

This is the second paragraph of the dissertation abstract, which will talk broadly about chapter 2: run timing forecast models.

This is the second paragraph of the dissertation abstract, which will talk broadly about chapter 3: in-season MSE models.

This is the third paragraph of the dissertation abstract, which will talk broadly about chapter 4: multi-stock population dynamics models and the best ways to inform management trade-offs.

Acknowledgments

Here is where I will thank everyone:

Catalano, Coggins, Connors, Jones, Dobson, Farmer, Fleischman, Smith, Liller, Esquible, Bechtol, Spaeder, Decossas, AL-HPC folks, Auburn Hopper HPC folks. Folks at the lab. Family and Michelle. RStudio staff. Martyn Plummer for JAGS. Instructors: Abebe (complex quant problems), Stevison (Shell/bash/HPC), McGowan (SDM), Sawant (GIS).

Table of Contents

Abstract	ii
Acknowledgments	iii
List of Figures	vi
List of Tables	x
1 Assessment Approaches for Single-Species, Mixed-stock Pacific Salmon Fisheries: Empirical and Simulation-Evaluation Applications	1
Abstract	1
1.1 Introduction	2
1.2 Methods	5
1.2.1 Multi-stock spawner-recruit models	6
1.2.2 Kuskokwim empirical analysis	13
1.2.3 Simulation-estimation trials	16
1.2.4 Computation	18
1.3 Results	19
1.3.1 Kuskokwim River empirical analysis	19
1.3.2 Simulation-estimation trials	27
1.4 Discussion	29
A Preparation of Data for Fitting Spawner-Recruit Models to Substocks of Kuskok- wim River Chinook Salmon in Chapter 1	60
A.1 Overview of data needs	60
A.2 Substock escapement	61
A.2.1 Spatial expansion	62

A.2.2	Temporal Expansion	63
A.3	Aggregate harvest	64
A.4	Age composition	65
A.5	Brood table reconstruction	66
A.6	Results	67
	A.6.1 Escapement	67
	A.6.2 Harvest	68
	A.6.3 Age composition	68
B	Simulation of Substock- and Year-Specific Maturity Schedules	75
B.1	Single substock, single year example	75
B.2	Extention to multiple substocks and years	76
	Bibliography	79

List of Figures

1.1	Visualization of how different types of heterogeneity in substock productivity and size influence the shape of trade-offs in mixed-stock salmon fisheries. Solid black lines are the case where stock types are split evenly among large/small and productive/unproductive stocks. Dotted black lines are the case where all small stocks are productive and all large stocks are unproductive, and dashed lines are the opposite (, all big stocks are productive). (a) Equilibrium aggregate harvest and proportion of substocks overfished plotted against the exploitation rate (b) value of the biodiversity objective (0 = all stocks overfished) plotted against the value of harvest (the long term proportion of the aggregate MSY attained). Notice that when all big stocks are productive (dashed lines), the trade-off is steeper, i.e., more harvest must be sacrificed in order to ensure a greater fraction of substocks are not overfished.	42
1.2	Map of the Kuskokwim River drainage, with the 13 drainage basins representing unique spawning units (substocks) used in this analysis. Black points show the location of weir projects, black sections of river indicate the reaches flown as part of aerial surveys. Drainages monitored via both aerial survey and weir used the weir counts to inform escapement estimates in this analysis, with the exception of the Aniak drainage (4), for which aerial survey data were much more abundant than the weir data.	43
1.3	Observed and fitted escapement time series for each Kuskokwim River substock. Line/symbol types denote the particular state-space model and grey squares denote observed data.	44
1.4	Observed and fitted harvest time series aggregated across all Kuskokwim River substocks included in this analysis. Line/symbol types denote the particular state-space model and grey squares denote observed data.	45
1.5	Observed and fitted age composition for the 6 weir-monitored substocks. Each scatter plot is the pair of fitted <i>versus</i> observed proportion of the escapement in each age each year with data available and the grey line represents the 1:1 perfect fit line. Point types denote two models: SSM-Vm (time-constant maturity; hollow circles) and SSM-VM (time-varying maturity; filled circles). \overline{ESS}_t represents the average number of fish successfully aged each year with data for each substock, which was used as the sample size to weight the data in the multinomial likelihoods that used these data. Panels are scaled to have the same <i>x</i> -axis and <i>y</i> -axis limits within an age across substocks and range from 0 – 1 for ages 4 – 6 and 0 – 0.3 for age 7.	46

1.6	Fit of the regression approaches to fitting the multi-stock spawner-recruit analysis to the Kuskokwim River substock data. Points are observed log(recruits/spawner) <i>versus</i> spawners, solid lines represent the fit for the independent regression models, and dashed lines represent the fit suggested by the model with random intercept effects for each substocks. Three substocks had fewer than 3 observed data points, rendering fitting a regression line infeasible. Note that a constraint was imposed that maintained $\log(\alpha_j) > 0$ which prevented biologically implausible values, and explains the poor fit for the Holokuk River substock.	47
1.7	Fitted spawner-recruit relationships for the 13 substocks monitored in the Kuskokwim River subdrainage included in this analysis. Line and point types correspond to different models; crosses are completely-observed spawner-recruit pairs. Note that the regression approaches (grey lines/triangles) fitted only to these data, the state-space models (black lines/circles) fitted to all observations of substock-specific escapement, aggregate harvest, and age composition.	48
1.8	Relationships between substock size and productivity as estimated by the 6 estimation approaches in the analysis. Symbol shapes denote the region within the Kuskokwim drainage the substock is located in and hollow symbols in the state-space models are substocks that could not be fitted by the regression approaches. The value in parentheses is Pearson's r correlation coefficient; bold numbers indicate a significant correlation at $\alpha = 0.05$	49
1.9	Correlation coefficients between recruitment residuals for each substock-pair. The size of each circle represents the magnitude of the correlation, color represents significance (whether 95% credible interval includes 0), and fill represents directionality as described in the legend. Substocks are ordered from downriver to upriver on both axes, and vertical/horizontal lines denote the boundaries between lower, middle, and upper river substocks.	50
1.10	Time series of recruitment residuals for each substock under each of the four state-space models. Substock-specific time series are represented by grey lines and the average across substocks within a brood year are represented by the thick black line. A dashed line at zero (no error) is provided for reference.	51
1.11	Visualization of harvest-biodiversity trade-offs based on equilibrium states (escapement and harvest) of the aggregate stock and the percentage of substocks expected to be in an undesirable state as a function of the exploitation rate under the assumption that all substocks are fished at the same rate. Overfished is defined here as $U > U_{MSY,j}$. "T.T." stands for "trending toward", and represents the case where equilibrium escapement would be ≤ 0 . To facilitate comparisons with the regression approaches (grey lines/triangles), the 3 substocks with insufficient data for fitting regression models were excluded from summaries of the state-space models (black triangles/circles).	52

1.12 Alternative (and more direct than Figure 1.11) visualization of harvest-biodiversity trade-offs for monitored Kuskokwim River Chinook salmon substocks. The conditions of overfished and trending towards extinction are the same as defined in Figure 1.11. These figures should be interpreted by determining how the value of the biodiversity objective (y -axis; expressed as the fraction of substocks that would not be in the undesirable condition) must be reduced to increase the value of the harvest objective (y -axis; expressed as a fraction of the maximum sustainable yield). To facilitate comparisons with the regression approaches (grey lines/triangles), the 3 substocks with insufficient data for fitting regression models were excluded from summaries of the state-space models (black triangles/circles). All symbols represent increasing exploitation rates in increments of 0.1 as you move down the y -axis.	53
1.13 Alternative vulnerability schedule (v_j) used in a sensitivity analysis of the state-space models. Vulnerabilities were obtained by determining the fraction of total fishing households the individual substocks must swim past in order to reach their respective natal spawning grounds. Substocks are ordered from downstream to upstream.	54
1.14 Difference in substock-specific parameter estimates between the alternative and default vulnerability schedules. Positive differences indicate that the alternative estimates were larger than the default estimates. Estimates are displayed for SSM-VM only, all other state-space models returned similar differences.	55
1.15 Difference in substock-specific parameter estimates between the alternative and default age composition weighting schemes. Positive differences indicate that the alternative estimates were larger than the default estimates. Filled symbols denote substocks with age composition data. Estimates are displayed for SSM-VM only, all other state-space models returned similar differences.	56
1.16 Central tendency and variability in proportional error for some parameters in the multi-stock spawner-recruit models from the simulation-estimation trials. Point estimates used were posterior medians.	57
1.17 Central tendency and variability in proportional error for some abundance states in the multi-stock spawner-recruit models from the simulation-estimation trials. Quantities are separated by the early portion of the time series (left panels) and the entire time series (right panels). Point estimates used were posterior medians.	58
1.18 Central tendency and variability in proportional error for key biological reference points of the aggregate mixed stock. S_p^* and U_p^* are the aggregate escapement and fully-vulnerable exploitation rate that would ensure no more than $p \cdot 100\%$ of substocks are overfished, respectively. Point estimates used were posterior medians.	59

A.1	The frequency of escapement sampling for each substock sampled in the Kuskokwim River. Black points indicate years that were sampled for substocks monitored with a weir and grey points indicate years sampled for substocks monitored with aerial surveys. The vertical black line shows a break where > 50% of the years were monitored for a stock.	72
A.2	The relationship between spatially-expanded aerial survey estimates and weir counts during the same years and substocks as described by (A.8). Notice the uncertainty expressed in the predictor variable; this was included in the analysis by incorporating both the spatial (Section A.2.1) and temporal (Section A.2.2) expansions in a single model fitted using Bayesian methods.	73
A.3	Estimated Chinook salmon escapement for substocks within the Kuskokwim River drainage. ‘Drainage-wide’ refers to the aggregate population estimates provided by a maximum likelihood run reconstruction model. ‘This analysis’ refers to the estimated portion of the aggregate run included in this analysis (not all tributaries have been monitored).	74
B.1	Simulated probability of maturation-at-age for 13 simulated substocks over time. Note the highly correlated patterns in year-specific variability.	78

List of Tables

1.1	Summary of evaluated models in this analysis. Regression models are described in Section 1.2.1.1 and state-space models are described in Section 1.2.1.2	30
1.2	Description of the various indices used in the description of the state-space model. n_t is the number of years observed for the most data-rich stock.	31
1.3	Prior distributions used for regression-based spawner-recruit parameters as described in Section 1.2.1.1. Prior distributions were identical for the empirical data and simulation-based analyses.	32
1.4	Prior distributions used for all model parameters in the state-space models. In all cases, priors were selected to be minimally-informative while still preventing the sampler from exploring highly unlikely areas of the parameter space. Differences between versions of the state-space model (e.g., SSM-vm and SSM-Vm; Table 1.1) are described by footnotes. Prior distributions were identical for the empirical data and simulation-based analyses.	33
1.5	Dimensions for the Markov Chain Monte Carlo algorithms used in this analysis. Note that the state-space models were sampled much more intensively than the regression models – this was to ensure adequate convergence and effective sample size for inference. Fewer chains were used for the simulation analysis to maximize High Performance Computing efficiency. MCMC diagnostics indicated these settings were adequate for reliable inference; the state-space models fitted to the empirical data were over-sampled to ensure this.	34
1.6	Estimated population parameters for Kuskokwim River Chinook salmon compared between assessment models, including the regression-based estimators. Only 10 of the 13 substocks had enough data to fit the linear regression model, the three missing stocks were discarded in the calculation of the summaries presented for the state-space models. Numbers shown are posterior medians with 95% credible limits in parentheses. Quantities with a bar and a j subscript denote averages over substocks, those with no subscript are the appropriate reference points for the aggregate of the 10 substocks.	35

1.7	Estimated population parameters and biological reference points for Kuskokwim River Chinook salmon compared between the four evaluated versions of the state-space assessment model assessment models. Unlike in Table 1.6, all 13 of the substocks were included in the calculation of these summaries. Numbers shown are posterior medians with 95% credible intervals in parentheses. Quantities with a bar and a j subscript denote averages over substock-specific parameters. Reference points with no subscript are the appropriate reference points for the aggregate of the 13 substocks included.	36
1.8	Comparison of management quantities obtained from the sensitivity analysis of the state-space model with regards to substock vulnerability. The default case had all substocks equally-vulnerable; the alternative case is shown in Figure 1.13, and reference points were calculated using the same vulnerability schedules as used in estimation. Estimates shown are from SSM-VM only, the other three models showed similar differences. The biodiversity metrics are expressed as the proportion of substocks expected to be overfished or trending towards extirpation at the mixed-stock MSY.	37
1.9	Comparison of management quantities obtained from the sensitivity analysis of the state-space model with regards to weighting of age composition data. Estimates shown are from SSM-VM only, the other three models showed similar differences. The biodiversity metrics are expressed as the proportion of substocks expected to be overfished or trending towards extirpation at the mixed-stock MSY.	38
1.10	Number of successful model fits and elapsed time for each multi-stock spawner-recruit analysis method from the simulation-estimation exercise. All regression-based methods were fitted in a single JAGS model. Subscripts denote differences in time units.	39
1.11	MCMC diagnostic summaries from the simulation-estimation trials. Numbers in the cells represent the percentage of all estimated values that did not meet a diagnostic threshold. For the Gelman-Rubin statistic, failure was defined as having a value of 1.1 or greater. For the effective samples, having fewer than 3,000 was considered a failure. According to the diagnostic by Raftery and Lewis (1992), 3,000 effective samples should result in a 99% chance of estimating the 0.025 or 0.975 posterior quantiles within ± 0.0125 quantile units, and a 83% chance of estimating the posterior median with the same level of precision. Diagnostic summaries are shown only if that parameter was assigned a prior in the model, e.g., regression-based models estimated α_j and β_j as leading parameters, whereas the state-space models estimated $U_{MSY,j}$ and $S_{MSY,j}$ as leading parameters.	40
1.12	Posterior coverage for key quantities in the simulation-estimation trials. Coverage was calculated as the percentage of all estimated 95% credible intervals across simulated data sets that contained the true quantity. Bold numbers are those that fall greater than 5 percentage points from the optimal coverage.	41

A.1 The estimated spatial expansion factors for the various aerial survey projects described in Section A.2.1. p_i represents the average fraction of telemetry tags that were detected outside of index flight reaches, which was used as the basis for determining the multiplier $(1 + \psi_i)$ needed to correct the aerial count for not flying the entire subdrainage. In cases where multiple projects were flown to count fish within one substock (e.g., the Aniak, see Figure 1.2 substock 4), the expanded project counts were summed to obtain an estimate for the total substock, as indicated by the footnotes.	70
A.2 The estimated temporal expansion parameters for converting spatially-expanded aerial counts to estimates of subdrainage-wide escapement abundance each year.	71

Chapter 1

Assessment Approaches for Single-Species, Mixed-stock Pacific Salmon Fisheries: Empirical
and Simulation-Evaluation Applications

Abstract

1.1 Introduction

Many salmon populations in large drainage systems are commonly harvested in a relatively small spatial area and are managed as a single stock. However, these “stocks” are instead stock-complexes, in which the aggregate stock is comprised of several (and sometimes, many) substocks. These substocks are known to show differences in genotypic (Templin et al. 2014), phenotypic (e.g., morphology; Hendry and Quinn 1997), behavioral (e.g., run timing; Clark et al. 2015; Smith and Liller 2017a,b), and life history (e.g., age-at-maturation, Blair et al. 1993) characteristics that are the result of adaptations to local environments after many generations of high spawning-site fidelity and reproductive isolation from conspecifics in other tributaries located within the same basin. It has been widely proposed that maintaining this diversity of local adaptation (hereafter, “biodiversity”) is favorable both from ecosystem and exploitation perspectives. One argument is that in a system where many parts contribute to the whole, the variability in the aggregate characteristics can be damped because of a lack of cohesion in the subcomponent dynamics, a phenomenon known as the “portfolio effect” (Schindler et al. 2010, 2015).

Variability in substock-specific characteristics can ultimately lead to heterogeneity in productivity among the substock components (Walters and Martell 2004). Productivity in this context is the ability of a population to replace itself after harvesting, often represented for salmon populations as the maximum number of future migrating adults (recruits) produced by one spawner (hereafter, α), which is attained at low spawner abundances due to density-dependent survival. Substocks j with higher α_j values can sustain greater exploitation rates (U) than those with smaller α_j values, in fact, α_j can be expressed in terms of the exploitation rate that maximizes sustained yield from substock j ($U_{\text{MSY},j}$; Schnute and Kronlund 2002):

$$\alpha_j = \frac{e^{U_{\text{MSY},j}}}{1 - U_{\text{MSY},j}}. \quad (1.1)$$

Given that there is likely some level of heterogeneity in α_j and $U_{\text{MSY},j}$ among individual substocks, the logical conclusion is that in a mixed-stock fishery where the exploitation rate in year t (U_t) is common among all substocks, some weaker substocks must be exploited at $U_t > U_{\text{MSY},j}$ in order to fish the more productive substocks at $U_{\text{MSY},j}$. This of course implies a trade-off, such that it may be necessary to over-exploit some substocks in order to maximize harvest (Figure 1.1, Walters and Martell 2004).

Before these trade-offs can be considered by managers in a well-informed way, the shape and magnitude of the trade-off must first be quantified as shown in Figure 1.1. Figures like this are generated using the estimated productivity and carrying capacity of all (or a representative sample) of the substocks within a mixed-stock fishery. These quantities are obtained using a spawner-recruit analysis, which involves tracking the number of recruits produced in each brood year (i.e., parent year) by the number of fish that spawned in that same year and fitting a curve to the resulting pattern. The spawner-recruit literature is extensive, but focuses primarily on assessing single populations as opposed to substock components (but see the work on Skeena River, British Columbia sockeye salmon *O. nerka* substocks; Walters et al. 2008; Korman and English 2013). Substock-specific analyses are uncommon because of two factors: (1) the data to conduct well-informed substock-specific spawner-recruit analyses are often unavailable (20 – 30 years of continuous spawner and harvest counts/estimates and age composition for each substock) and (2) management actions in large mixed-stock fisheries may not be dexterous enough to deliberately exert higher exploitation rates on more productive substocks, so deriving substock-specific estimates could be of little utility. Regarding the former reason, there are some cases where the data do exist to perform these kinds of analyses, however methods to conduct multi-stock spawner-recruit analyses are not well-developed. Regarding the latter, even in cases where management cannot target particular substocks over others, understanding the nature of the trade-offs can

be informative for evaluating candidate harvest policies for the mixed-stock in the context of substock biodiversity (Walters et al. 2018).

The methods to fit spawner-recruit models can be grouped into two broad categories: regression-based approaches (e.g., Clark et al. 2009) and state-space (i.e., time series) models (e.g., Su and Peterman 2012; Fleischman et al. 2013). The regression-based approaches treat spawner-recruit pairs as independent observations, and are thus subject to substantial pitfalls when dealing with (1) the inherent time-dependent properties and (2) oftentimes large amounts of observation error found in spawner-recruit data sets (Walters and Martell 2004, Ch. 7). The consequence of ignoring the first issue is the “time-series bias”, which chronically causes positive biases in α and negative biases in β , resulting in the same directional biases in U_{MSY} and S_{MSY} , respectively (i.e., spuriously providing too aggressive harvest policy recommendations; Walters 1985). The second is known as the “errors-in-variables bias” and is known to cause an apparent scatter which inserts additional variability that commonly-used regression estimators do not account for (Ludwig and Walters 1981). Though these methods have been known for their problems for over 30 years, they are still somewhat widely used (Korman and English 2013). Unlike the regression-based approaches, the state-space class of models captures the process of recruitment events leading to future spawners while simultaneously accounting for variability in the biological and measurement processes that gave rise to the observed data (de Valpine and Hastings 2002; Fleischman et al. 2013). For these reasons, state-space spawner-recruit analyses have been rapidly gaining popularity, particularly in Alaska (Su and Peterman 2012; Fleischman et al. 2013; Staton et al. 2017). Including this level of additional model complexity comes at computational costs, as these models are well-suited for Bayesian inference with Markov Chain Monte Carlo (MCMC) methods (Newman et al. 2014, Ch. 4), but has been shown to reduce bias in estimates in some circumstances (Su and Peterman 2012; Walters and Martell 2004).

In the Kuskokwim River Chinook salmon fishery, there has been recent interest in considering biodiversity to explicitly inform the drainage-wide escapement goal. In conducting the spawner-recruit analysis to inform such policy analyses, it will be difficult to determine which method is appropriate, given many possible model structures, sparse data, and unknown sampling biases. Before strong inferences can be made from the ultimate trade-off analyses of interest, the performance of the estimation models used to parameterize them needs to be evaluated, as well as the appropriate level of model complexity needed to address the problem with sufficient accuracy. In this chapter, I evaluate the performance of a range of assessment models for mixed-stock salmon fisheries *via* simulation-estimation. The objectives were to:

- (1) develop a set of varyingly-complex multi-stock versions of state-space spawner-recruit models,
- (2) determine the sensitivity of biological and trade-off conclusions to assessment model complexity (including those obtained using regression-based approaches) using empirical data from Kuskokwim River Chinook salmon substocks, and
- (3) test the performance of the assessment models *via* simulation-estimation trials.

1.2 Methods

This analysis was conducted in both an empirical and a simulation-estimation framework to evaluate the sensitivity and performance of assessment strategies for the mixed-stock assessment problem in Pacific salmon fisheries. First, all assessment methods (2 regression-based and 4 state-space models) were fitted to observed data from the Kuskokwim River substocks ($n_j = 13$) to determine the extent to which the choice of assessment model structure might influence biological and management conclusions. Then, a hypothetical system was generated with known properties and was composed of several age-structured substocks. Then, these hypothetical populations were sampled per a realistic sampling scheme and each of the assessment models were fitted to the resulting data sets. Estimation performance

regarding quantities used in management (e.g., U_{MSY} and S_{MSY}) was calculated from the resulting estimates. Inference from the simulation can then be used to justify an appropriate level of model complexity for this problem when applied to the Kuskokwim and systems like it.

1.2.1 Multi-stock spawner-recruit models

1.2.1.1 Regression-based models

Two regression-based approaches to estimating Ricker (1954) spawner-recruit parameters in the multi-stock case were assessed: (1) a single mixed-effect regression model with random intercepts and (2) independent regression models. The Ricker (1954) spawner-recruit model can be written as:

$$R_y = \alpha S_y e^{-\beta S_y + \varepsilon_y} \quad (1.2)$$

where R_y is the total recruitment expected to be produced by the escapement S_y in brood year y , α is the maximum expected recruits-per-spawner (RPS), β is the inverse of the escapement that is expected to produce maximum recruitment (S_{MAX}), and ε_y are independent mean zero random variables attributed solely to environmental fluctuations. Primary interest lies in estimating the population dynamics parameters α and β as they can be used to obtain biological reference points off of which sustainable harvest policies can be developed. This function is increasing at small escapements and declining at large ones, though can be linearized:

$$\log(\text{RPS}_y) = \log(\alpha) - \beta S_y + \varepsilon_y, \quad (1.3)$$

allowing for estimation of the parameters $\log(\alpha)$ and β in a linear regression framework using the least squares method (Clark et al. 2009). This relationship is nearly always declining,

implying a compensatory effect on survival (i.e., RPS) with reductions in spawner abundance (Rose et al. 2001).

It is not difficult to conceive a multi-stock formulation of this model by including substock-specific random effects on the intercept [$\log(\alpha)$]:

$$\begin{aligned}\log(\text{RPS}_{y,j}) &= \log(\alpha_j) - \beta_j S_{y,j} + \varepsilon_y, \\ \log(\alpha_j) &= \log(\alpha) + \varepsilon_{\alpha,j}, \\ \varepsilon_{\alpha,j} &\sim N(0, \sigma_\alpha).\end{aligned}\tag{1.4}$$

It does not make sense to include substock-level random effects on the slope, given that β is a capacity parameter related to the compensatory effect of resource limitation experienced by juveniles, likely in the freshwater environment (i.e., amount of habitat as opposed to quality of habitat). Fitting the individual substock models in this hierarchical fashion allows for the sharing of information such that the more intensively-assessed substocks can help inform those that are more data-poor.

The mixed-effect model may have the benefit of sharing information to make some substocks more estimable, but it should also have the tendency to pull the extreme α_j (those in the tails of the hyperdistribution) toward α . This behavior may not be preferable for policy recommendations, as it should tend to dampen the extent of heterogeneity estimated in α_j . For this reason, independent regression estimates for each substock were obtained also for evaluation. In estimating the parameter $\log(\alpha)$, a lower bound constraint of 0 was used in all regression models. This was necessary to prevent the models from estimating biologically-impossible parameters: if $\log(\alpha) < 0$, then the stock would produce < 1 RPS at its most productive state, in which case it would likely not currently be in existence.

1.2.1.2 State-space models

Four versions of the state-space formulation were developed. As 3 versions were simplifications of the full model, the full model is presented completely here and the changes resulting in the other 3 model structures are described following the description of the full model.

The state-space formulation of a multi-stock spawner-recruit analysis developed and evaluated here is an extension of various single-stock versions (e.g., Fleischman et al. 2013). Walters et al. (2008) used a similar model using maximum likelihood methods to provide estimates of >50 substocks in the Skeena River drainage, British Columbia. The model presented here was fitted in the Bayesian mode of inference using program JAGS (Plummer 2017), and allows for relaxation of certain assumptions made by Walters et al. (2008) such as the important notion of perfectly-shared recruitment residuals (i.e., anomalies – deviations from the expected population response). It also has the ability to relax the assumption of constant maturity schedules across brood years. See Table 1.2 for a description of the index notation, in particular note the difference between the brood year index y and the calendar year index t .

The state-space model is partitioned into two submodels: (1) the process submodel which generates the true states of $R_{y,j}$ and the resulting calendar year states (e.g., $S_{t,j}$) and (2) the observation submodel which fits the true states to the observed data. Note that this method allows for missing calendar year observations and does not require excluding brood year recruitment events that were not fully-observed as was necessary for the regression-based models (see Appendix A.5).

The recruitment process operated by producing a mean prediction from the deterministic Ricker (1954) relationship (1.2) for n_y brood years for each of the n_j substocks. From these deterministic predictions, auto-correlated process variability was added to generate the true realized state. To populate the first n_a calendar year true states with recruits of each age a , the first a_{max} brood year expected recruitment states were not linked to a spawner abundance

through (1.2) (because the S_y component was not observed), but instead were assumed to have a constant mean equal to the unfished equilibrium recruitment (where non-zero S_j produces $R_j = S_j$ when unexploited and in the absence of process variability):

$$\bar{R}_{y,j} = \frac{\log(\alpha_j)}{\beta_j}, \quad (1.5)$$

where $\bar{R}_{y,j}$ is the expected (i.e., deterministic) recruitment in brood year y from substock j with Ricker parameters α_j and β_j . The remaining $n_y - a_{max}$ brood years had an explicit time linkage:

$$\bar{R}_{y,j} = \alpha_j S_{t,j} e^{-\beta_j S_{t,j}}, \quad (1.6)$$

where $t = y - a_{max}$ is the t^{th} calendar year index in which the escapement produced the recruits in the y^{th} brood year index.

From these deterministic predictions of the biological recruitment process, lag-1 auto-correlated process errors were added to produce the true realized states:

$$\log(R_{y,1:n_j}) \sim \text{MVN} \left(\log(\bar{R}_{y,1:n_j}) + \omega_{y,1:n_j}, \Sigma_R \right), \quad (1.7)$$

where

$$\omega_{y,1:n_j} = \phi \left(\log(R_{y-1,1:n_j}) - \log(\bar{R}_{y-1,1:n_j}) \right), \quad (1.8)$$

and $R_{y,1:n_j}$ is a vector of true recruitment states across the n_j stocks in brood year y , $\omega_{y,1:n_j}$ is the portion of the total process error attributable to serial auto-correlation, ϕ is the lag-1 auto-correlation coefficient (constant across substocks), and Σ_R is a covariance matrix representing the white noise portion of the total recruitment process variance. Σ_R was estimated such that each substock was assigned a unique variance and covariance with each other substock. This

was achieved by using an inverse Wishart prior distribution, with degrees of freedom equal to $n_j + 1$ and the scale matrix populated with zero-value elements along the off-diagonals and 1 along the diagonal elements, which inserts little information about the covariance matrix Σ_R (Plummer 2017). The multivariate normal errors were on the logarithmic scale so the variability on $R_{y,j}$ was lognormal, which is the most commonly used error distribution for describing spawner-recruit data sets (Walters and Martell 2004). Further, the multivariate normal was used as opposed to n_j separate normal distributions so the degree of synchrony in brood year recruitment deviations (i.e., recruitment process errors) among substocks could be captured and freely estimated.

The maturity schedule is an important component of age-structured spawner-recruit models, as it determines which calendar years the brood year recruits $R_{y,j}$ return to spawn (and be observed). Recent state-space spawner-recruit analyses have accounted for brood year variability in maturity schedules as Dirichlet random vectors drawn from a common hyperdistribution characterized by a mean maturation-at-age probability vector ($\pi_{1:n_a}$) and an inverse dispersion parameter (D) (see Fleischman et al. 2013; Staton et al. 2017, for implementation in JAGS), and the same approach was used here with maturity schedules shared perfectly among substocks within a brood year. Brood year-specific maturity schedules were treated as random variables such that:

$$p_{y,a} \stackrel{\text{iid}}{\sim} \text{Dirichlet}(\pi_{1:n_a} D). \quad (1.9)$$

where $p_{y,a}$ is the probability a fish spawned in brood year y will mature at age a .

In order to link $R_{y,j}$ with calendar year observations of escapement from each substock, $R_{y,j}$ was allocated to calendar year runs-at-age ($N_{t,a,j}$) based on the maturity schedule:

$$N_{t,a,j} = R_{t+n_a-a,j} p_{t+n_a-a,a}, \quad (1.10)$$

and the total run returning to substock j in year t was the sum across ages:

$$N_{t,j} = \sum_{a=1}^{n_a} N_{t,a,j}. \quad (1.11)$$

The harvest process was modeled using a freely estimated annual exploitation rate (U_t) time series, which was assumed to apply equally to all substocks:

$$H_{t,j} = N_{t,j} U_t, \quad (1.12)$$

and escapement was obtained as:

$$S_{t,j} = N_{t,j} (1 - U_t). \quad (1.13)$$

The quantity H_t aggregated among all substocks was obtained by summing $H_{t,j}$ within a t index across the j indices. The true age composition returning in year t to substock j ($q_{t,a,j}$) was obtained as:

$$q_{t,a,j} = \frac{N_{t,a,j}}{N_{t,j}}. \quad (1.14)$$

Three data sources were used to fit the model: (1) observed escapement from each substock ($S_{obs,t,j}$) with assumed known coefficients of variation (CV), (2) total harvest arising from the aggregate stock ($H_{obs,t}$) with assumed known CV, and (3) the age composition of substocks with these data each calendar year ($q_{obs,t,a,j}$; which had associated effective sample size $ESS_{t,j}$ equal to the number of fish successfully aged for substock j in year t). The CVs were converted to lognormal standard deviations:

$$\sigma_{\log} = \sqrt{\log(CV^2 + 1)}, \quad (1.15)$$

and used in lognormal likelihoods to fit the time series $S_{t,j}$ to $S_{obs,t,j}$ and H_t to $H_{obs,t}$. Calendar year age composition was fitted using multinomial likelihoods with parameter vectors $q_{t,1:n_a,j}$ and observed vectors of $(q_{obs,t,1:n_a,j} ESS_{t,j})$.

Three alternative formulations of the state-space model were evaluated, and all were simplifications of the full model described above regarding the structure of (1) the covariance matrix on recruitment residuals and (2) the maturity process (see Table 1.1 for a summary). The simplest model did not include brood year variability in maturity schedules and Σ_R was constructed by estimating a single σ_R^2 and ρ , and populating the diagonal elements with σ_R^2 and off-diagonal elements with $\rho\sigma_R^2$. This simplest model is denoted as SSM-vm throughout the rest of this chapter. One drawback of constructing Σ_R this way is that $\rho < -0.05$ for a 13×13 covariance matrix results in positive-indefiniteness, which is prohibited by JAGS (Plummer 2017). Thus, a constraint was required to maintain $-0.05 \leq \rho < 1$ to prevent the sampler from crashing. In one intermediate model (SSM-vM), brood year maturation variability was included but the covariance matrix was constructed as in the simplest model. In the other intermediate model (SSM-Vm), brood year variability in maturation was not included but the covariance matrix was fully estimated as in the full model (SSM-VM). As for the choice of notation, lowercase letters indicate the simple version of a structure and uppercase letters indicate the complex structure; “v” refers to recruitment covariance structure and “m” refers to maturity. These models were chosen for the simple *versus* complex comparisons because these are two key areas where an analyst might question if the data are adequate for model fitting and inference. In other words, these are two key structural uncertainties where it is important to know if the complex versions are reliably estimable with a reasonable amount of data.

1.2.2 Kuskokwim empirical analysis

1.2.2.1 Study system

All six assessment models (2 regression-based and 4 state-space models) developed in this chapter were fitted to empirical data from Chinook salmon substocks of the Kuskokwim River located in western Alaska (Figure 1.2). The Kuskokwim River salmon fishery can very well be described as a mixed-stock fishery, both for multiple salmon species (predominately Chinook, chum *O. keta*, and sockeye salmon) and for multiple substocks of the same species. Fish originating from and returning to the various tributaries enter through the bulk of the fishery as a mixed-stock, though Chinook salmon stocks traveling to the headwaters have been illustrated to enter the main stem earliest in the summer migration (Smith and Liller 2017a,b) so a limited ability to direct harvest toward or away from these substocks is possible by manipulating the front portion of the fishery (Chapter ??, this dissertation). It is acknowledged that the assessment program does not sample all tributaries within the Kuskokwim River where Chinook salmon spawn, but total run size between 1976 – 2017 has been estimated *via* run reconstruction (Liller et al. 2018).

1.2.2.2 Data sources

The data set used that included counts of Chinook salmon at many locations throughout the Kuskokwim River system. Nearly all data were collected by projects managed by the Alaska Department of Fish and Game (ADF&G) and a complete description of data needs and preparation procedures is provided in Appendix A. The raw escapement data set available spanned 20 different escapement monitoring projects (6 weirs and 14 aerial surveys) and 42 calendar years from 1976 – 2017; some pre-processing was required to convert the aerial survey index counts to estimates of total spawners (Appendix A.2). Annual estimates of Chinook salmon harvest originating from both subsistence and commercial fisheries in each

year was also available, as was the estimated exploitation rate of the aggregate stock (details in Appendix A.3). Finally, age composition data were available for the 6 substocks monitored *via* weir programs (details in Appendix A.4).

1.2.2.3 Sensitivity Analyses

Two sensitivity analyses were conducted to test the robustness of inference from the state-space models with the Kuskokwim data. First, the default assumption that all substocks have been fished at the same rate each year is tenuous. I included in the model a term that allowed for substocks to have differential vulnerability (v_j) by replacing U_t with $U_t v_j$ in (1.12) and (1.13) which makes an adjustment that acknowledges some substocks may have been fished harder in the past. This alteration changes the interpretation of the parameter vector U_t to be the exploitation rate of fully-vulnerable substocks. Without additional information on what portion of $H_{obs,t}$ was attributable to each substock going back in time, the v_j elements are not estimable. In the absence of this information for Kuskokwim River Chinook salmon, an alternative vulnerability schedule was generated by calculating the fraction of the fishing households substocks must travel past in order to reach their natal spawning grounds. Fishing household data were available from post-season interviews conducted by ADF&G (e.g., Hamazaki 2011; Shelden et al. 2016)¹. Although this method ignores the temporal overlap of the fishery (Hamazaki 2008) with the arrival timing of particular substock groups (Smith and Liller 2017a,b), it was intended as a first step at determining how much the conclusions might depend on how the internal harvest accounting was specified. No attempt was made to alter how harvest was apportioned for use in the regression-based models.

As a secondary sensitivity analysis, the information content of the age composition data was reduced. In the default case, each multinomial vector was weighted by the number of fish successfully aged for that substock/year combination. For some substocks/years, this number

¹These data were the same as those used in Chapter ?? of this dissertation when determining the spatial distribution of fishing effort and salmon needs in the management strategy evaluation operating model.

was quite high from a multinomial sampling perspective when the number of categories is small (e.g., $\approx 1,200$ samples across 4 age categories). To assess whether this strength of information had an impact on the inference, I manipulated the effective sample size such that the maximum number of fish sampled for a substock was assigned $ESS_{t,j} = 100$, and the other years with data were scaled proportionately.

1.2.2.4 Comparisons of model output

Key population dynamics parameters and biological reference points were compared between 6 six assessment models wherever possible to determine the extent to which the management conclusions might change based on the model structure used. Where appropriate, quantities were averaged across substocks to facilitate comparisons and included indicators of the average substock's productivity ($\bar{\alpha}_j$ and $\bar{U}_{MSY,j}$) and size ($\bar{S}_{eq,j}$, $\bar{S}_{MSY,j}$, and $\bar{S}_{MAX,j}$). Reference points for the aggregate mixed-stock included U_{MSY} and S_{MSY} and a set of metrics that incorporate biodiversity aspects as well: S_p^* , H_p^* , and U_p^* , which represent the mixed-stock escapement, harvest, or exploitation rate, respectively, that would ensure no more than $p \cdot 100\%$ of substocks would be overfished, defined here as the case where a substock would be fished at $U > U_{MSY,j}$. Three levels of p were extracted: 0.1, 0.3, and 0.5.

The output of the state-space models allowed much richer biological interpretations of substock dynamics, and comparisons between models can be informative about the extent to which biological conclusions depend on the assumed model structure. Model fits to the data ($S_{obs,t,s}$, $H_{obs,t}$, and $q_{obs,t,a,j}$) were examined for all state-space models and noteworthy differences between model structures were identified. Estimates of synchrony in recruitment anomalies were examined, both between two average substocks ($\bar{\rho}_{i,j}$), and between all substock pairs. For the simple recruitment variance models (SSM-vm and SSM-vM), correlations between each substock pair were conducted by applying Pearson's r coefficient to two substocks' estimated recruitment anomaly time series; in the complex variance models these

correlations were captured in the freely-estimated covariance matrix, and they were extracted and summarized. Although the state-space models were ignorant of the spatial relationships between the substocks, comparisons were made to determine if substocks closer in proximity showed higher synchrony than those spaced more distantly, as might be expected. The auto-correlation parameter (ϕ) and characteristics of the maturity schedules (π_a and D) were also compared between state-space models.

Harvest biodiversity trade-offs were visualized in two ways. First, the equilibrium aggregate mixed-stock escapement and harvest were calculated² at each level of a mixed-stock exploitation rate that affected all substocks equally. The fraction of substocks overfished and trending towards extirpation (defined as the case where $S_{eq,U,j} \leq 0$) were also calculated. As a secondary, possibly more direct trade-off visualization, the fraction of substocks overfished and trending towards extirpation was plotted against the fraction of the mixed-stock MSY obtained at each exploitation rate.

Some substocks could not be fitted using the regression approach because they had fewer than three observed pairs of $RPS_{y,j}$ (see Appendix A.5 for details). When comparing quantities to the estimates from the state-space models, the substocks that could not be fitted with the regression approaches were removed from the state-space model outputs. When comparisons were made between state-space models only, these substocks were retained.

1.2.3 Simulation-estimation trials

To test the performance of these models, I created 160 hypothetical salmon data sets designed to mimic the Kuskokwim River empirical data set. I attempted to fit each of the 6 estimation models described in Section 1.2.1 to each data set.

²Equilibrium equations for the Ricker (1954) model can be found in Table 2 of Schnute and Kronlund (2002) for the case where $\gamma = 0$.

Given that the state-space model is a much more natural model of this system (which has intrinsic time series properties) than the regression-based versions, it was used as the foundation of the operating model (i.e., state-generating model). The biological submodel was more complex than the most complex estimation model – namely in regards to the maturity schedule, which had a modest level of substock variability in mean maturity but with highly correlated brood year variability; see Appendix B for details. In order to serve as the state-generating model for the simulation, the state-space model needed only to be populated with true parameters, initial states, and a harvest control rule. A fixed exploitation rate policy was used (chosen to maximize yield without overfishing more than 30% of the substocks) with a modest amount of implementation error to ensure the data time series were generated with enough contrast in spawner abundance. $n_j = 13$ substocks were simulated with different parameters $U_{\text{MSY},j}$ and $S_{\text{MSY},j}$ which took on the values of random posterior draws from the most complex state-space model fitted to the Kuskokwim River Chinook salmon substock data. All other parameters were chosen to mimic the estimated values from the Kuskokwim analysis, with the exception of Σ_R , which was set to have a modest amount of substock recruitment variability ($\bar{\sigma}_{j,j} \approx 0.4$); $\rho_{i,j}$ for each pair of substocks was simulated randomly between -1 and 1, but approximately 0 when averaged across all substocks.

For a given set of simulated true states, a set of observed states ($S_{\text{obs},t,j}$, $H_{\text{obs},t}$, $q_{\text{obs},t,a,j}$) was generated by adding sampling error to each year, which represented the value that would have been observed if the sampling project operated that year. Observation errors in escapement and harvest estimates were lognormal and multinomial for the age composition, as assumed in the state-space estimation model. Frequency of sampling on each substock (i.e., simulated data collection) was set to approximately mimic the Kuskokwim River historical monitoring program (Figure A.1). The sampling frequency was designed to continue to generate sampling schedules until one was found that ensured no substock had fewer than 3 observations of $RPS_{y,j}$ which allowed the regression-based models to include all substocks.

Aggregate harvest ($H_{obs,t}$) was assumed to be available every year in each simulation and it was assumed that the exploitation rate could be estimated in an unbiased fashion.

Estimation performance in terms of accuracy between assessment models was calculated using the proportional error ($\frac{x_{est}-x_{true}}{x_{true}}$), and the central tendency and variability between random data sets were visualized using boxplots. Key quantities of interest for comparison between the regression approaches and the state-space models included: S_{MSY} , U_{MSY} , S_p^* , U_p^* , α_j , $U_{MSY,j}$, and $S_{MSY,j}$. For the state-space models, the ability to accurately estimate the abundance states of $R_{y,j}$, $S_{t,j}$, and H_t was also assessed, summarized for early years and all years separately to investigate the influence of the assumption that the observation time series began at unfished equilibrium, as described by (1.5). Credible interval coverage at the 95% level was assessed by determining what fraction of obtained credible intervals included the true value. Additionally, model run times and convergence diagnostics were summarized for all models that successfully fitted the simulated data sets.

1.2.4 Computation

All parameter estimation was conducted in the Bayesian framework using the MCMC engine JAGS (Plummer 2017) invoked through R (R Core Team 2018) using the package `{jagsUI}` (Kellner 2017). All priors for the regression-based methods (Table 1.3) and state-space models (Table 1.4) were selected to be as minimally-informative as possible, while still preventing the MCMC sampler from exploring highly unlikely areas of the parameter space. I wrote two packages to simplify the workflow of this analysis³: one to handle the generation of simulated age-structured salmon populations from a mixed-stock fishery (`{SimSR}`; Staton 2018c) and one to handle the fitting and summarization of model output (`{FitSR}`; Staton 2018b). The former is one that other researchers may find useful for streamlining salmon

³For reference, any of the packages I wrote for this analysis can be installed on any R user's computer by executing: `devtools::install_github("bstaton1/pkgname")`.

population dynamics studies, whereas the later is highly specific to this particular analysis (in terms of the models included). Additionally, I made extensive use of another package I had previously written for summarizing the output of JAGS models, which other researchers using JAGS may find useful (`{codaTools}`; Staton 2018a).

See Table 1.5 for details on the MCMC sampling specifications used for all models. Posterior convergence was assessed using visual inspection of the MCMC sampling behavior and the convergence diagnostic proposed by Brooks and Gelman (1998). Adequate sampling was further verified for key estimated quantities using the effective sample size and the Raftery-Lewis diagnostic (Raftery and Lewis 1992). All posterior distributions were summarized using the median and 95% equal-tailed credible intervals. In cases where a quantity was averaged over substocks or years (e.g., $\bar{\alpha}_j$), the average was calculated for each joint posterior sample, then the resulting marginal posterior of the average was summarized.

As a result of the long required model run times and the large number of simulated salmon data sets (i.e., replicates) for the simulation study, this analysis required more computing power than the previous chapters. I conducted this analysis using High Performance Computing services provided by the Alabama Supercomputer Authority. This allowed me to run many jobs at once, where each job fitted one model to one data set using one processor core for each chain in parallel. In this way, I was able to complete just over 3 years of computing time (if each job was ran back-to-back) in less than 1 month (as a result of many parallel jobs).

1.3 Results

1.3.1 Kuskokwim River empirical analysis

1.3.1.1 State-space models fit to data

In general, the four state-space models produced the same escapement state time series, especially in years with data (represented by the grey squares; Figure 1.3). For several

substocks, there were no escapement data prior to the mid-1990s, and this is one area the various state-space models produced different escapement estimates. In the early portion of the time series, the models with brood year variability in maturity included (SSM-vM and SSM-VM) tended to estimate higher escapement abundance than the models with time-constant maturity (SSM-vm and SSM-Vm). For example, substocks spawning in the Kwethluk, George, Holokuk, and Takotna rivers all showed this pattern (Figure 1.3).

There were several cases where extremely high (and seemingly unrealistic) escapement states were estimated by the state-space model, though these only occurred in the versions with simple maturation schedules (Figure 1.3). The period in the late-1980s and the early-1990s had much (i.e., 5 – 10 times) higher estimated escapement than ever observed for the Holitna, Pitka, and Tatlawiksuk substocks under either models SSM-vm or SSM-Vm. The George River substock had abnormally large escapements in the mid-1990s, and was again most exaggerated for the SSM-vm and SSM-Vm versions. All of these cases occurred when no escapement data were available; in years with data all state-space models fitted the escapement data quite well (Figure 1.3).

In general, the fit to the aggregate harvest data was good (Figure 1.4), though the time-varying maturity schedule versions (SSM-vM and SSM-VM) fitted the data nearly perfectly. The constant maturity schedule versions resulted in a harvest state that was greater than twice as large as the observed state in 1976 (the first observed year). These models did not show discrepancies nearly this large for the rest of the time series (Figure 1.4). Note the precipitous decline in harvest starting in the late-2000s, which coincides with a nearly decade-long period of low productivity for this stock.

Just as for the escapement and harvest data, the state-space models generally fitted the age data well. The only differences between model structures came in the distinction between how maturity was treated. The complex maturity models had visually-better fit than the simple maturity models (Figure 1.5) for most substocks and ages. This difference in fit was

most exaggerated for substocks that had the most fish aged each year (e.g., the Kogrukuk and Kwethluk substocks; Figure 1.5).

1.3.1.2 Regression models fit to data

Ten of the 13 substocks had sufficient data to fit the regression models (≥ 3 brood year spawner-recruit pairs): those spawning in the Kisaralik, Oskawalik, and Holitna subdrainages. In general, the two regression approaches provided similar fits to the data. At least 5 substocks had essentially equal fitted lines between approaches (Figure 1.6). Only two substocks showed major discrepancies between the fitted relationships: the Holokuk and the Pitka substocks. For the Holokuk relationship, the three data points suggested a negative intercept and an increasing slope (Figure 1.6), however the intercepts of these models were constrained to be positive to prevent biological impossibilities ($\alpha_j < 1$), which explains the poor fit in this case.

1.3.1.3 Spawner-recruit dynamics comparisons

There were large discrepancies between the suggested population productivity parameters between the regression models and the state-space models (Table 1.6). For these comparisons, I removed the 3 substocks that could not be fitted by the regression approaches from the summaries of the state-space models. Both regression approaches suggested the maximum productivity of the average substock ($\bar{\alpha}_j$) was far higher than any of the state-space models. The independent regression approach provided an estimate of $\bar{\alpha}_j = 7.74$ (4.47 – 19.97) and the mixed-effect regression approach suggested $\bar{\alpha}_j = 4.62$ (3.15 – 7.56). Most state-space models suggested $\bar{\alpha}_j < 3$, with the highest upper 95% credible limit being 4.92, obtained by SSM-vM (Table 1.6).

These patterns are well-illustrated at the substock-level by plotting the expected recruitment at each spawner abundance for each model (Figure 1.7). It is evident that the four state-space models behaved similarly near the origin (which is governed by α_j), whereas in

many cases the regression models suggested steeper slopes near the origin (corresponding to higher values of α_j). State-space models tended to disagree with one another more at larger spawner abundances (Figure 1.7), suggesting that inferences about stock size and the strength of compensation are dependent on the details how recruitment variance and maturity are modeled for some substocks. As would be expected, the mixed-effect regression approach differed from the independent regression estimates the most for substocks with fewer observations (e.g., Pitka *versus* Kogrukuk; Figure 1.7).

These differences in estimated productivity translated directly to the maximum sustainable exploitation rate for the average substock ($\bar{U}_{\text{MSY},j}$): the independent and mixed-effects regression approaches resulted in estimates of 0.58 (0.46 – 0.68) and 0.51 (0.41 – 0.6), respectively, whereas the point estimates ranged from 0.36 – 0.45 across the state-space models (Table 1.6). In terms of the exploitation rate that would maximize yield from the aggregate mixed stock (U_{MSY}), the regression approaches suggested the stock should be fished quite hard to obtain MSY (as high as $U_{\text{MSY}} = 0.78$ for the independent regression approach), whereas all state-space models suggested $U_{\text{MSY}} < 0.5$ for point estimates and no 95% credible intervals exceeded 0.65 (Table 1.6).

In comparing the state-space model estimates from these 10 substocks to the complete set of 13 substocks, the average productivity and maximum sustainable exploitation rates were quite similar, indicating the stocks with insufficient data for regression were missing at random in these regards (compare the rows corresponding to $\bar{\alpha}_j$, $\bar{U}_{\text{MSY},j}$, and U_{MSY} between Tables 1.6 and 1.7).

One metric of substock size is the spawner abundance expected to exactly replace itself under unfished equilibrium conditions ($S_{\text{eq},j}$). When averaged across substocks, the regression approaches suggested the Kuskokwim River substocks were approximately 2,500 fish smaller than the state space models did (Table 1.6). The other metrics used for measuring substock size ($S_{\text{MAX},j}$ and $S_{\text{MSY},j}$) followed the same pattern: smaller values for the regression

approaches than the state-space models, though the magnitude varied depending on the metric (larger discrepancies found for $\bar{S}_{\text{MAX},j}$ than $\bar{S}_{\text{MSY},j}$. $\bar{S}_{\text{MAX},j}$ was 70% larger for state-space models with time-constant maturity schedules (approximately 16,500) than models with time-varying maturity (approximately 9,500; Table 1.6). In terms of the aggregate mixed stock escapement expected to produce maximum sustained yield (S_{MSY}), regression approaches suggested much smaller escapements were necessary than the state-space models; by a margin of 10,000 – 15,000 fish (Table 1.6). In comparing the uncertainty in S_{MSY} between state-space models, those with time-constant maturity schedules had much more uncertainty than the time-varying models (i.e., wider credible limits; Table 1.6).

In comparing the state-space model estimates from these 10 substocks to the complete 13 substocks, the average substock-specific size metrics were fairly similar, indicating the stocks with insufficient data for regression were missing at random in this regard (compare the rows corresponding to $\bar{S}_{\text{eq},j}$, $\bar{S}_{\text{MAX},j}$, and $\bar{S}_{\text{MSY},j}$ between Tables 1.6 and 1.7). In terms of the aggregate reference point S_{MSY} , the estimates were quite different – which should be expected given some substocks' abundance and production were excluded from Table 1.6 and included in Table 1.7. With all substocks included, the estimate was approximately 40,000 compared to approximately 30,000 when they were excluded – indicating escapement from the Holitna, Kisaralik, and Oskawalik should make up approximately 25% of the escapement amongst the substocks included in this analysis if the management objective was to maximize long-term yield.

As illustrated in Figure 1.1, the relationship between substock size and productivity matters for policy conclusions about trade-offs. I examined the relationship between substock size (represented by $S_{\text{eq},j}$) *versus* productivity (represented by $U_{\text{MSY},j}$) for the Kuskokwim River substocks (Figure 1.8). Both regression approaches suggested reasonably strong patterns between substock size (Pearson's correlation r coefficient of 0.43 and 0.54 for the independent and mixed-effects approaches, respectively, though $p < 0.05$ for both approaches). The

state-space models generally suggested weaker or absent relationships between substock size and productivity, except for SSM-VM, which had an r value of 0.56 that was statistically-significant at the $\alpha = 0.05$ level. The state-space models suggested that upper-river substocks were mostly smaller than average, but were made of both productive and unproductive substocks, whereas most of the larger substocks are located in the middle river (relatively speaking; Figure 1.8).

In terms of recruitment variability, the regression-based approaches suggested that the average standard deviation of the lognormal distribution that describes randomness in the recruitment process ($\bar{\sigma}_{R,j}$) was 0.78 and 0.52 for the independent and mixed-effects versions, respectively (Table 1.6). The state-space models estimated that the average amount of recruitment process variability by substock was quite a bit higher: point estimates ranged from 0.85 – 1.11 (Table 1.6). The models with time-varying maturity had estimates on the lower end of this range, which is explained by the inclusion of an additional biological process that could describe variability in the data.

Unlike the regression models, the state-space models estimated the degree of covariance between substock recruitment residuals. All the state-space models estimated a moderate amount of correlation in recruitment variance (i.e., synchrony) between two average substocks ($\bar{\rho}_{i,j}$): point estimates ranged between 0.18 – 0.28, and none of the models suggested 95% credible limits that encompassed 0, indicating there is evidence to suggest some degree of positive synchrony between the Kuskokwim River substocks. The simple variance models (SSM-vm and SSM-vM) estimated a single correlation parameter, whereas the complex versions (SSM-Vm and SSM-VM) estimated a unique value for each substock combination. The estimated correlation of realized recruitment residual pairs between substocks is displayed in Figure 1.9. One might expect that substock pairs belonging in the same region might show higher degrees of synchrony than substock pairs in different regions, though this analysis suggested this was not necessarily the case (the state-space models were unaware of the spatial

relation between substocks). Large correlations (e.g., >0.5) were found between lower-upper combinations, lower-lower, and upper-upper substocks (Figure 1.9). Relatively few large correlations were found between middle river substocks with other substocks, though both SSM-Vm and SSM-VM suggested that the Holokuk and Oskawalik substocks have highly synchronous recruitment dynamics, which is interesting given their close proximity (Figure 1.2; substocks #5 and #6, respectively). Conversely, all models suggested the Holitna and Kogrukuk substocks have little synchrony, and they fall within the same subdrainage (Figure 1.2; substocks #7 and #8, respectively). Most correlations were positive, especially those that were large in magnitude (Figure 1.9). A notable exception was the correlation between the Kisaralik substock and the Holokuk and Oskawalik substocks: their dynamics were suggested to be largely opposite.

A visualization of the consequences of these patterns for the recruitment residual time series is shown in Figure 1.10. As would be expected, the models with only one correlation parameter (SSM-vm and SSM-vM) showed greater synchrony in time trends between substocks (especially SSM-vM) than the models with complex correlation structure. There was a weak cycling tendency of favorable and poor recruitment conditions (Figure 1.10), which is consistent with the degree of estimated lag-1 auto-correlation in each time series (ϕ ; range across state-space models: 0.27 – 0.33; no credible intervals encompassed 0; Table 1.7).

The only difference in mean maturity schedule estimates came in the comparison between models with and without time-varying maturity (and the differences were slight; Table 1.7). The models that allowed time-varying maturity suggested that the inter-brood year variability was quite high ($D \approx 18$; Table 1.7).

1.3.1.4 Trade-off comparisons

With increasing mixed-stock exploitation rates, the aggregate equilibrium escapement declined, but did so more rapidly for the state-space models than the regression models (Figure

1.11). State-space models that included time-varying maturity suggested higher equilibrium escapement and harvest would be available at most exploitation rates than models with time-constant maturity. Regression models suggested that MSY was much larger and occurred at a higher exploitation rate than for the state-space models, as would be expected based on comparing the estimated population dynamics parameters between these methods (Table 1.6). In terms of biodiversity, the time-varying maturity models suggested fewer substocks would be overfished or trending towards extirpation at low exploitation rates than the time-constant maturity models, and the regression approaches suggested even more optimistic conclusions (Figure 1.11).

Another and more direct way of visualizing the trade-off between harvest and biodiversity suggested the trade-off conclusions are nearly identical between state-space models in terms of substock overfishing and slight differences in terms of substocks trending towards extirpation (Figure 1.12). The state-space models suggested that in order to maximize yields, approximately half of the substocks would need to be overfished and approximately a fifth would be trending towards extinction (Figure 1.12). The regression approaches suggested a more pessimistic conclusion: approximately 80% of substocks would need to be overfished to attain MSY. These patterns were the same even if only 60% of MSY was desired, though less exaggerated (Figure 1.12).

1.3.1.5 Sensitivity analyses

The alternative vulnerability schedule (v_j) based on the spatial distribution of fishing households resulted in lower river substocks (those spawning in the Kwethluk, Kisaralik, and Tuluksak rivers) having the lowest v_j ranging between 0.7 – 0.8, the middle river substocks ranging between 0.9 and 0.95, and those in the upper river between 0.95 and 1 (Figure 1.13). Most changes in substock specific $U_{MSY,j}$ and $S_{eq,j}$ were negligible (± 0.05) (Figure 1.14), and most (8 of 13) substocks showed increases in $U_{MSY,j}$. Changes in $U_{MSY,j}$ occurred

randomly with respect to changes in vulnerability: some substocks in the three regions showed both increases and decreases (Figure 1.14). With respect to substock size ($S_{eq,j}$), upper river substocks showed increases of approximately 100 fish and lower river substocks showed decreases of between 100 and 1,000 fish. Middle river substocks showed a mix of increases and decreases in $S_{eq,j}$, with the largest change 1,000 fish in the Holitna river substock (Figure 1.14). Derived biological reference points for the aggregate mixed-stock showed a high degree of similarity as well: escapement-related quantities were ~3,000 fish smaller and harvest-related quantities were ~3,000 fish larger for the alternative vulnerability schedule, however the conclusions about substock biodiversity at MSY were nearly identical (Table 1.8).

The alternative age composition weighting resulted in more substantial differences from the default case. Twelve of the 13 substocks saw increases of between 0.03 – 0.14 in $U_{MSY,j}$ and most $S_{eq,j}$ were estimated to be between 500 and 1,200 fish smaller when the alternative scheme was used (Figure 1.15). Derived biological reference points for the aggregate mixed-stock differed as well: escapement-related quantities were ~6,000 – 10,000 fish smaller and harvest-related quantities were ~6,000 – 12,000 fish larger for the alternative vulnerability schedule, however the conclusions about substock biodiversity at MSY still were nearly identical (Table 1.8).

1.3.2 Simulation-estimation trials

State-space models took between 1.3 and 2.9 days to fit on average, with longer run times associated with more complex models (Table 1.10) and the regression-based models took less than an hour in all cases. The state-space models fitted successfully to the majority of simulated data sets (~140 out of 160) and the regression-based models were fitted successfully in all cases (Table 1.10). No attempts were made to try different initial values for the ~20 data sets that failed in fitting for the state-space models, though because they were generally

the same data sets that failed across state-space models, this was likely a characteristic of the data sets. MCMC diagnostics suggested that the vast majority of models converged and that enough samples were retained for adequate inference (Table 1.11).

Regression models were found to systematically overestimate the substock-specific quantities of α_j and $U_{MSY,j}$ and in some cases they produced wildly erroneous estimates. The mixed-effect model was more accurate than the method that fitted independent regressions to each substock (Figure 1.16). State-space models far more accurately and precisely estimated these productivity-based quantities than the regression-approaches, though there was still a slight positive bias (median proportional error $\approx 5\%$; Figure 1.16). Additionally, regression approaches tended to underestimate $S_{MSY,j}$ more than the state-space models. All state-space models tended to overestimate $\sigma_{R,j}$ by approximately 5% regardless of the assumed covariance structure, though the degree of serial auto-correlation (ϕ) was accurately estimated. The individual state-space models showed essentially no differences for these quantities (Figure 1.16). However, models with simple covariance structure tended to overestimate the correlation between substocks and *vice versa* for the complex covariance structure.

The state-space model was a largely unbiased estimator of abundance-related states ($R_{y,j}$, $S_{t,j}$, and H_t). The early portion of the time series had a slight tendency to be overestimated (Figure 1.17), likely a result of the assumption that data collection began when the substocks were unfished.

Just as for the substock-specific quantities, the regression-based methods provided generally poorer estimates of mixed-stock biological reference points than state-space models and there was no loss in performance with state-space model complexity (Figure 1.18). The mixed-effect regression produced more positively-biased estimates of $U_{0.1}^*$ and $U_{0.3}^*$ than the independent regression approach, but this pattern switched for $U_{0.5}^*$ and U_{MSY} , likely as a result of the estimated shape of the distribution of substock productivity. The mixed-effect version was less dispersed, meaning that productivities in the lower tail would have been

closer to the mean (i.e., larger) than for the independent regression approach. State-space models tended to produce slight underestimates of $U_{0.1}^*$ and $U_{0.3}^*$ and slight over estimates of $U_{0.5}^*$ and U_{MSY} (Figure 1.18).

Credible interval coverage was better for the state-space models than for regression approaches. For substock-specific parameters, the regression approaches had lower coverage than the state-space models and the models that had the complex recruitment variance structure had more parameters close to the optimal level of 95% (Table 1.12). All state-space models had low coverage for π which resulted from highly narrow credible intervals, not from inaccurate estimates. In terms of mixed-stock biological reference points, the state-space model provided much better coverage than the regression approaches, particularly for exploitation rate-based points (Table 1.12). All state-space models exhibited poor coverage for abundance-related states (Table 1.12).

1.4 Discussion

Here's what it means.

Table 1.1: Summary of evaluated models in this analysis. Regression models are described in Section 1.2.1.1 and state-space models are described in Section 1.2.1.2

Abbreviation	n_j	Unique σ_j	AR(1)	Shared Recruitment Dynamics
Regression-Based Models				
LM	10	Yes	No	Independent residuals
LME	10	No	No	Independent residuals
State-Space Models				
vm	13	No	Yes	Single ρ bounded by [-0.05 – 1)
Vm	13	Yes	Yes	Unique $\rho_{i,j}$
vM	13	No	Yes	Same as vm
VM	13	Yes	Yes	Same as Vm

Table 1.2: Description of the various indices used in the description of the state-space model.
 n_t is the number of years observed for the most data-rich stock.

Index	Meaning	Dimensions
y	Brood year index; year in which fish were spawned	$n_y = n_t + n_a - 1$
t	Calendar year index; year in which observations are made	n_t
j	Substock index	n_j
a	Age index; $a = 1$ is the first age; $a = n_a$ is the last age	n_a
a_{min}	The first age recruits can mature	1
a_{max}	The last age recruits can mature	1

Table 1.3: Prior distributions used for regression-based spawner-recruit parameters as described in Section 1.2.1.1. Prior distributions were identical for the empirical data and simulation-based analyses.

Parameter	Prior
Independent Regression Models	
$\log(\alpha_j)$	Uniform(0, 5)
β_j	Uniform(0, 1)
$\sigma_{R,j}$	Uniform(0, 5)
Mixed-Effect Regression Model	
$\log(\alpha)$	Uniform(0, 10)
σ_α	Uniform(0, 10)
β_j	Uniform(0, 1)
σ_R	Uniform(0, 5)

Table 1.4: Prior distributions used for all model parameters in the state-space models. In all cases, priors were selected to be minimally-informative while still preventing the sampler from exploring highly unlikely areas of the parameter space. Differences between versions of the state-space model (e.g., SSM-vm and SSM-Vm; Table 1.1) are described by footnotes. Prior distributions were identical for the empirical data and simulation-based analyses.

Parameter	Prior	Description
$U_{\text{MSY},j}$	Uniform(0.01, 0.99)	Exploitation rate that produces MSY
$S_{\text{MSY},j}$	Lognormal(0, 0.001)	Spawner abundance that produces MSY
ϕ	Uniform(-0.99, 0.99)	Lag-1 auto-correlation coefficient
Σ_R^{-1} ^a	Wishart(R , $n_j + 1$)	Inverse covariance matrix for white-noise recruitment process variability
σ_R ^b	Uniform(0, 2)	White-noise recruitment process standard deviation
ρ ^b	Uniform(-0.05, 1)	Correlation in recruitment process variability among substocks
π	Dirichlet($\alpha = [1, 1, 1, 1]$)	Average probability of maturing at each age
$D^{-0.5}$ ^c	Uniform(0.03, 1)	Dispersion of brood year-specific maturity schedules
p_y ^c	Dirichlet($\alpha = \pi \cdot D$)	Brood year-specific probability of maturing at each age
U_t	Beta(1,1)	Annual exploitation rate of fully-vulnerable substocks

^a Only for SSM-Vm and SSM-VM

^b Only for SSM-vm and SSM-vM, Σ_R was constructed using σ_R and ρ as described at the end of Section 1.2.1.2.

^c Only for SSM-vM and SSM-VM, all p_y took on π for SSM-vm and SSM-Vm.

Table 1.5: Dimensions for the Markov Chain Monte Carlo algorithms used in this analysis. Note that the state-space models were sampled much more intensively than the regression models – this was to ensure adequate convergence and effective sample size for inference. Fewer chains were used for the simulation analysis to maximize High Performance Computing efficiency. MCMC diagnostics indicated these settings were adequate for reliable inference; the state-space models fitted to the empirical data were over-sampled to ensure this.

	Regression Models		State-Space Models	
	Empirical	Simulation	Empirical	Simulation
Burn-in	20,000	20,000	50,000	50,000
Post Burn-in	100,000	200,000	800,000	600,000
Thin Interval	50	50	400	100
Chains	10	5	10	5
Total	1,200,000	1,100,000	8,500,000	3,250,000
Saved	20,000	20,000	20,000	30,000

Table 1.6: Estimated population parameters for Kuskokwim River Chinook salmon compared between assessment models, including the regression-based estimators. Only 10 of the 13 substocks had enough data to fit the linear regression model, the three missing stocks were discarded in the calculation of the summaries presented for the state-space models. Numbers shown are posterior medians with 95% credible limits in parentheses. Quantities with a bar and a j subscript denote averages over substocks, those with no subscript are the appropriate reference points for the aggregate of the 10 substocks.

Parameter	Regression-Based Models			State-Space Models		
	LM	LME	vm	Vm	vM	VM
$\bar{\alpha}_j$	7.74 (4.47 – 19.97)	4.62 (3.15 – 7.56)	2.94 (1.92 – 4.95)	2.64 (1.87 – 3.92)	3.28 (2.25 – 4.92)	2.84 (2.02 – 4.03)
$\bar{U}_{MSY,j}$	0.58 (0.46 – 0.68)	0.51 (0.41 – 0.6)	0.39 (0.25 – 0.52)	0.36 (0.24 – 0.49)	0.45 (0.32 – 0.56)	0.4 (0.28 – 0.52)
Σ	$\bar{S}_{MSY,j}$ 2,500 (1,900 – 5,300)	2,600 (2,100 – 3,900)	3,700 (2,300 – 7,100)	4,200 (2,500 – 7,800)	3,500 (2,700 – 5,400)	3,700 (2,800 – 5,600)
	$\bar{S}_{MAX,j}$ 4,900 (3,200 – 21,200)	5,700 (3,900 – 22,500)	16,300 (7,400 – 83,800)	16,800 (7,800 – 64,100)	9,500 (5,900 – 42,700)	9,600 (6,100 – 26,400)
	$\bar{S}_{eq,j}$ 6,800 (5,200 – 13,300)	6,700 (4,100 – 9,400)	8,400 (5,200 – 15,600)	9,400 (5,600 – 17,200)	8,300 (6,400 – 12,300)	8,600 (6,600 – 12,600)
	$\bar{\sigma}_{R,j}$ 0.78 (0.56 – 1.15)	0.52 (0.44 – 0.65)	1.02 (0.9 – 1.17)	1.11 (0.91 – 1.33)	0.85 (0.75 – 0.98)	0.85 (0.73 – 1.01)
	U_{MSY} 0.78 (0.6 – 0.97)	0.68 (0.48 – 0.84)	0.43 (0.21 – 0.66)	0.4 (0.2 – 0.6)	0.48 (0.33 – 0.63)	0.45 (0.3 – 0.61)
	S_{MSY} 16,100 (4,100 – 33,200)	18,800 (8,700 – 32,200)	25,800 (8,800 – 64,300)	30,700 (10,700 – 73,100)	29,500 (17,300 – 45,300)	33,700 (19,700 – 50,900)

Table 1.7: Estimated population parameters and biological reference points for Kuskokwim River Chinook salmon compared between the four evaluated versions of the state-space assessment model assessment models. Unlike in Table 1.6, all 13 of the substocks were included in the calculation of these summaries. Numbers shown are posterior medians with 95% credible intervals in parentheses. Quantities with a bar and a j subscript denote averages over substock-specific parameters. Reference points with no subscript are the appropriate reference points for the aggregate of the 13 substocks included.

Parameter	vm	Vm	vM	VM
$\bar{\alpha}_j$	2.75 (1.91 – 4.35)	2.44 (1.78 – 3.5)	3.21 (2.25 – 4.66)	2.81 (2.03 – 4.18)
$\bar{U}_{MSY,j}$	0.37 (0.25 – 0.49)	0.33 (0.22 – 0.44)	0.44 (0.32 – 0.55)	0.39 (0.28 – 0.5)
$\bar{S}_{MSY,j}$	4,100 (2,700 – 6,900)	4,300 (2,600 – 8,200)	3,800 (2,900 – 6,000)	3,600 (2,800 – 5,900)
$\bar{S}_{MAX,j}$	16,700 (9,100 – 72,200)	19,300 (9,800 – 81,100)	10,400 (6,400 – 46,900)	10,000 (6,200 – 37,500)
$\bar{S}_{eq,j}$	9,300 (6,100 – 15,300)	9,500 (5,800 – 17,900)	9,000 (6,900 – 13,400)	8,500 (6,600 – 13,200)
$\bar{\sigma}_{R,j}$	1.02 (0.9 – 1.17)	1.25 (1.05 – 1.49)	0.85 (0.75 – 0.98)	0.99 (0.85 – 1.18)
$\bar{\rho}_{i,j}$	0.21 (0.1 – 0.36)	0.18 (0.09 – 0.31)	0.28 (0.15 – 0.44)	0.19 (0.09 – 0.32)
U_{MSY}	0.39 (0.23 – 0.59)	0.37 (0.19 – 0.57)	0.47 (0.32 – 0.62)	0.46 (0.31 – 0.63)
S_{MSY}	41,300 (16,400 – 81,900)	40,600 (13,800 – 93,300)	41,300 (24,900 – 64,300)	41,600 (23,300 – 64,200)
ϕ	0.33 (0.12 – 0.49)	0.32 (0.13 – 0.49)	0.27 (0.06 – 0.44)	0.3 (0.11 – 0.48)
π_1	0.27 (0.265 – 0.275)	0.271 (0.266 – 0.276)	0.232 (0.204 – 0.263)	0.234 (0.203 – 0.264)
π_2	0.379 (0.374 – 0.384)	0.379 (0.373 – 0.384)	0.371 (0.336 – 0.406)	0.372 (0.337 – 0.407)
π_3	0.327 (0.322 – 0.332)	0.327 (0.321 – 0.332)	0.359 (0.324 – 0.392)	0.357 (0.323 – 0.392)
π_4	0.024 (0.022 – 0.025)	0.024 (0.022 – 0.025)	0.037 (0.027 – 0.049)	0.037 (0.027 – 0.049)
D	—	—	17.95 (13.32 – 23.74)	18.28 (13.63 – 24.06)

Table 1.8: Comparison of management quantities obtained from the sensitivity analysis of the state-space model with regards to substock vulnerability. The default case had all substocks equally-vulnerable; the alternative case is shown in Figure 1.13, and reference points were calculated using the same vulnerability schedules as used in estimation. Estimates shown are from SSM-VM only, the other three models showed similar differences. The biodiversity metrics are expressed as the proportion of substocks expected to be overfished or trending towards extirpation at the mixed-stock MSY.

Quantity	v_j Schedule	
	Default	Alternative
Escapement		
$S_{0.1}^*$	85,300 (61,200 – 130,300)	83,500 (59,500 – 129,000)
$S_{0.3}^*$	68,800 (49,700 – 102,400)	66,700 (47,200 – 99,700)
$S_{0.5}^*$	51,300 (36,300 – 72,600)	48,800 (33,400 – 71,900)
S_{MSY}	41,600 (21,500 – 64,600)	41,800 (23,300 – 67,500)
Harvest		
$H_{0.1}^*$	17,800 (4,100 – 39,600)	20,600 (5,000 – 45,500)
$H_{0.3}^*$	27,100 (11,300 – 49,100)	30,300 (12,500 – 55,800)
$H_{0.5}^*$	33,100 (16,400 – 56,800)	36,100 (17,800 – 62,800)
MSY	34,900 (17,900 – 59,600)	37,500 (19,000 – 64,800)
Exploitation Rate		
$U_{0.1}^*$	0.17 (0.04 – 0.34)	0.2 (0.05 – 0.38)
$U_{0.3}^*$	0.28 (0.13 – 0.42)	0.32 (0.16 – 0.48)
$U_{0.5}^*$	0.39 (0.25 – 0.52)	0.44 (0.29 – 0.59)
U_{MSY}	0.46 (0.3 – 0.64)	0.5 (0.33 – 0.68)
$\bar{U}_{full,t}$	0.32 (0.42 – 0.35)	0.35 (0.48 – 0.41)
Biodiversity		
$p_{OF,\text{MSY}}$	0.62 (0.38 – 0.85)	0.62 (0.38 – 0.85)
$p_{EX,\text{MSY}}$	0.23 (0 – 0.62) ³⁷	0.23 (0 – 0.54)

Table 1.9: Comparison of management quantities obtained from the sensitivity analysis of the state-space model with regards to weighting of age composition data. Estimates shown are from SSM-VM only, the other three models showed similar differences. The biodiversity metrics are expressed as the proportion of substocks expected to be overfished or trending towards extirpation at the mixed-stock MSY.

Quantity	$ESS_{t,j}$ Scheme	
	Default	Alternative
Escapement		
$S_{0.1}^*$	85,300 (61,200 – 130,300)	75,600 (56,700 – 104,900)
$S_{0.3}^*$	68,800 (49,700 – 102,400)	59,900 (44,800 – 81,400)
$S_{0.5}^*$	51,300 (36,300 – 72,600)	42,700 (31,200 – 56,600)
S_{MSY}	41,600 (21,500 – 64,600)	35,000 (21,800 – 48,100)
Harvest		
$H_{0.1}^*$	17,800 (4,100 – 39,600)	24,100 (6,200 – 48,100)
$H_{0.3}^*$	27,100 (11,300 – 49,100)	36,200 (16,400 – 59,100)
$H_{0.5}^*$	33,100 (16,400 – 56,800)	44,700 (24,700 – 68,800)
MSY	34,900 (17,900 – 59,600)	46,600 (26,200 – 71,900)
Exploitation Rate		
$U_{0.1}^*$	0.17 (0.04 – 0.34)	0.24 (0.06 – 0.43)
$U_{0.3}^*$	0.28 (0.13 – 0.42)	0.38 (0.19 – 0.53)
$U_{0.5}^*$	0.39 (0.25 – 0.52)	0.51 (0.36 – 0.63)
U_{MSY}	0.46 (0.3 – 0.64)	0.57 (0.41 – 0.71)
$\bar{U}_{full,t}$	0.32 (0.42 – 0.35)	0.32 (0.41 – 0.34)
Biodiversity		
$p_{OF,\text{MSY}}$	0.62 (0.38 – 0.85)	0.62 (0.38 – 0.85)
$p_{EX,\text{MSY}}$	0.23 (0 – 0.62)	0.23 (0.08 – 0.54)

Table 1.10: Number of successful model fits and elapsed time for each multi-stock spawner-recruit analysis method from the simulation-estimation exercise. All regression-based methods were fitted in a single JAGS model. Subscripts denote differences in time units.

	# Data Sets		Elapsed Time		
	Attempted	Successful	Minimum	Mean	Maximum
LM + LME^a	160	158	4.8	10.9	21.6
SSM-vm^b	160	138	0.8	1.3	2.8
SSM-Vm^b	160	135	1.2	1.9	3.5
SSM-vM^b	160	139	1.2	2	4.1
SSM-VM^b	160	139	1.8	2.9	5.1

Time Units

^a Minutes

^b Days

Table 1.11: MCMC diagnostic summaries from the simulation-estimation trials. Numbers in the cells represent the percentage of all estimated values that did not meet a diagnostic threshold. For the Gelman-Rubin statistic, failure was defined as having a value of 1.1 or greater. For the effective samples, having fewer than 3,000 was considered a failure. According to the diagnostic by Raftery and Lewis (1992), 3,000 effective samples should result in a 99% chance of estimating the 0.025 or 0.975 posterior quantiles within ± 0.0125 quantile units, and a 83% chance of estimating the posterior median with the same level of precision. Diagnostic summaries are shown only if that parameter was assigned a prior in the model, e.g., regression-based models estimated α_j and β_j as leading parameters, whereas the state-space models estimated $U_{\text{MSY},j}$ and $S_{\text{MSY},j}$ as leading parameters.

Parameter	Gelman-Rubin						Effective MCMC Samples					
	Regression		State-space				Regression		State-space			
	LM	LME	vm	Vm	vM	VM	LM	LME	vm	Vm	vM	VM
α_j	<1	<1	—	—	—	—	<1	0	—	—	—	—
β_j	<1	0	—	—	—	—	<1	0	—	—	—	—
$U_{\text{MSY},j}$	—	—	0	0	0	0	—	—	<1	4	<1	4
$S_{\text{MSY},j}$	—	—	0	<1	0	0	—	—	<1	4	<1	5
$\sigma_{R,j}$	—	—	0	0	0	0	—	—	0	<1	0	<1
ϕ	—	—	0	0	0	0	—	—	0	0	0	0
π	—	—	0	0	0	0	—	—	0	0	0	0
$\bar{\rho}_{i,j}$	—	—	0	0	0	0	—	—	0	<1	0	0
$R_{y,j}$	—	—	0	<1	<1	<1	—	—	<1	<1	<1	<1
U_t	—	—	0	0	0	0	—	—	0	<1	0	<1

Table 1.12: Posterior coverage for key quantities in the simulation-estimation trials. Coverage was calculated as the percentage of all estimated 95% credible intervals across simulated data sets that contained the true quantity. Bold numbers are those that fall greater than 5 percentage points from the optimal coverage.

Quantity	Regression		State-space			
	LM	LME	vm	Vm	vM	VM
Parameters						
α_j	84	68	95	94	95	95
β_j	83	73	90	88	90	89
$U_{\text{MSY},j}$	84	68	95	94	95	95
$S_{\text{MSY},j}$	85	76	85	84	85	85
$\sigma_{R,j}$	—	—	44	93	45	94
ϕ	—	—	87	97	88	97
π	—	—	12	11	16	16
$\bar{\rho}_{i,j}$	—	—	87	93	88	93
Mixed-stock reference points						
$S_{0.1}^*$	99	94	93	92	93	93
$S_{0.3}^*$	99	94	96	95	96	96
$S_{0.5}^*$	94	91	91	90	91	90
S_{MSY}	100	87	94	90	94	92
$U_{0.1}^*$	79	37	96	97	96	96
$U_{0.3}^*$	66	32	99	99	99	99
$U_{0.5}^*$	20	37	95	95	96	96
U_{MSY}	75	80	95	92	95	93
Abundance states						
U_t	—	—	64	64	66	66
$R_{y,j}$	—	—	59	58	60	59
$S_{t,j}$	—	—	50	49	51	51
H_t	—	—	51	51	55	55

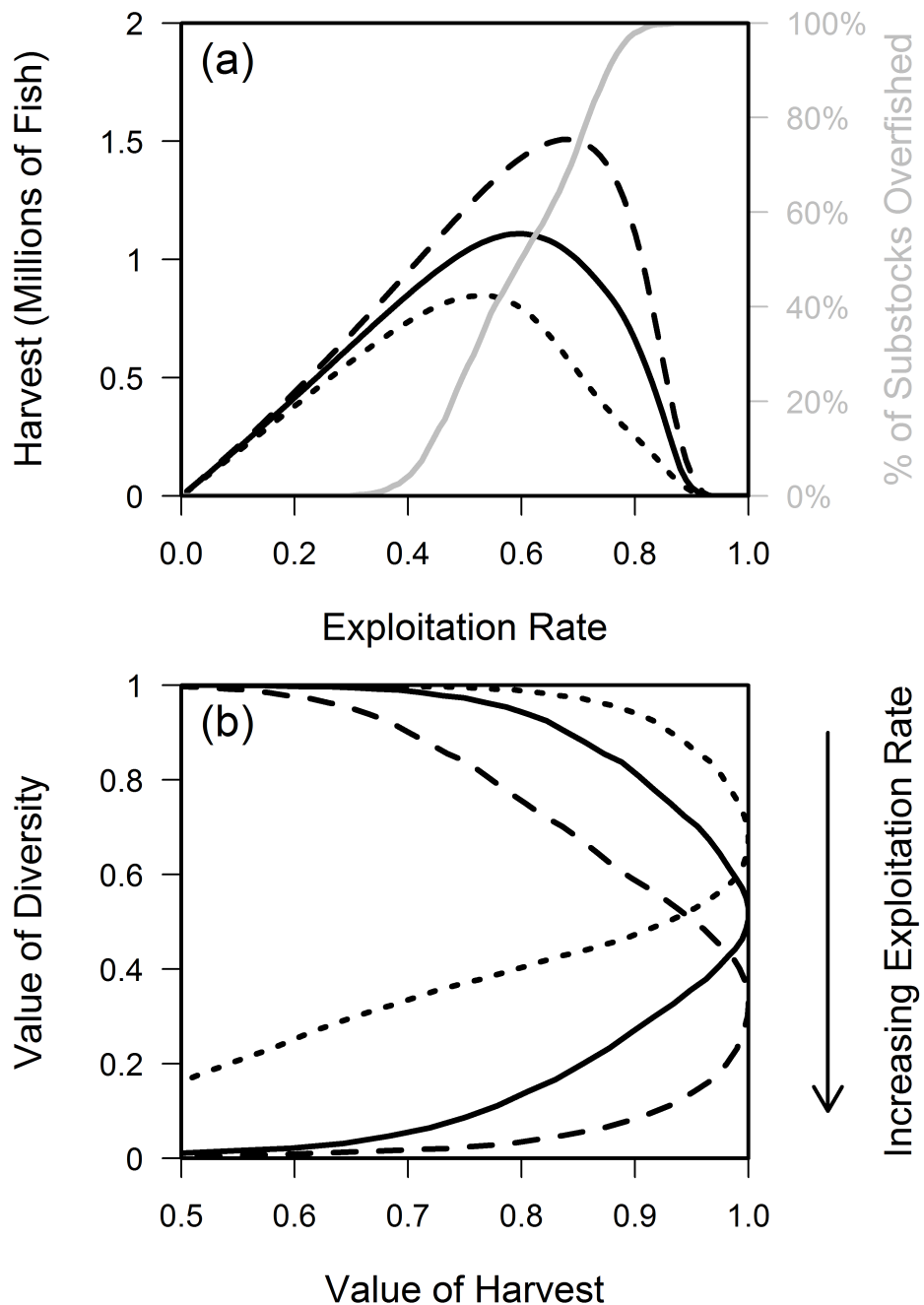


Figure 1.1: Visualization of how different types of heterogeneity in substock productivity and size influence the shape of trade-offs in mixed-stock salmon fisheries. Solid black lines are the case where stock types are split evenly among large/small and productive/unproductive stocks. Dotted black lines are the case where all small stocks are productive and all large stocks are unproductive, and dashed lines are the opposite (, all big stocks are productive). (a) Equilibrium aggregate harvest and proportion of substocks overfished plotted against the exploitation rate (b) value of the biodiversity objective (0 = all stocks overfished) plotted against the value of harvest (the long term proportion of the aggregate MSY attained). Notice that when all big stocks are productive (dashed lines), the trade-off is steeper, i.e., more harvest must be sacrificed in order to ensure a greater fraction of substocks are not overfished. ⁴²

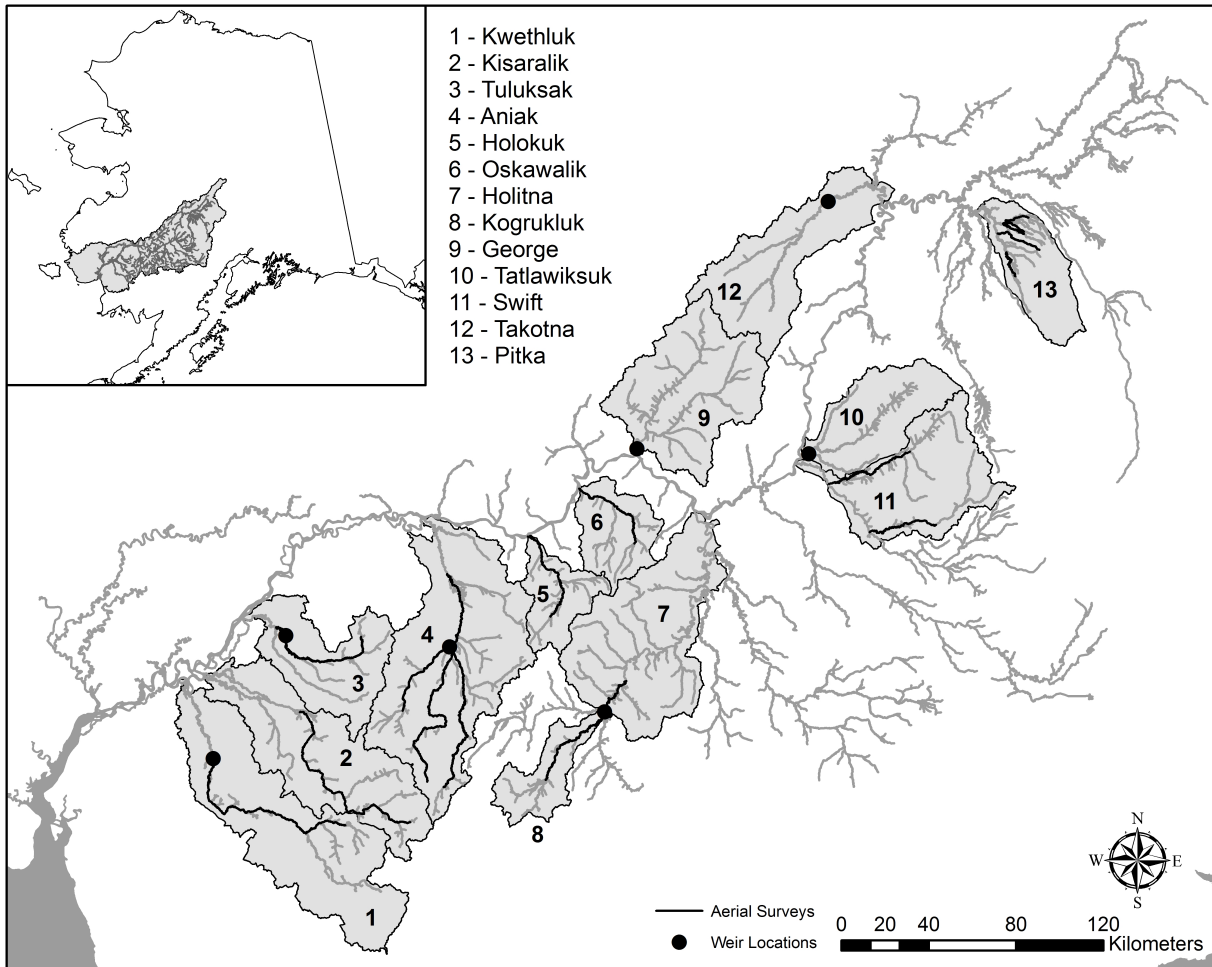


Figure 1.2: Map of the Kuskokwim River drainage, with the 13 drainage basins representing unique spawning units (substocks) used in this analysis. Black points show the location of weir projects, black sections of river indicate the reaches flown as part of aerial surveys. Drainages monitored via both aerial survey and weir used the weir counts to inform escapement estimates in this analysis, with the exception of the Aniak drainage (4), for which aerial survey data were much more abundant than the weir data.

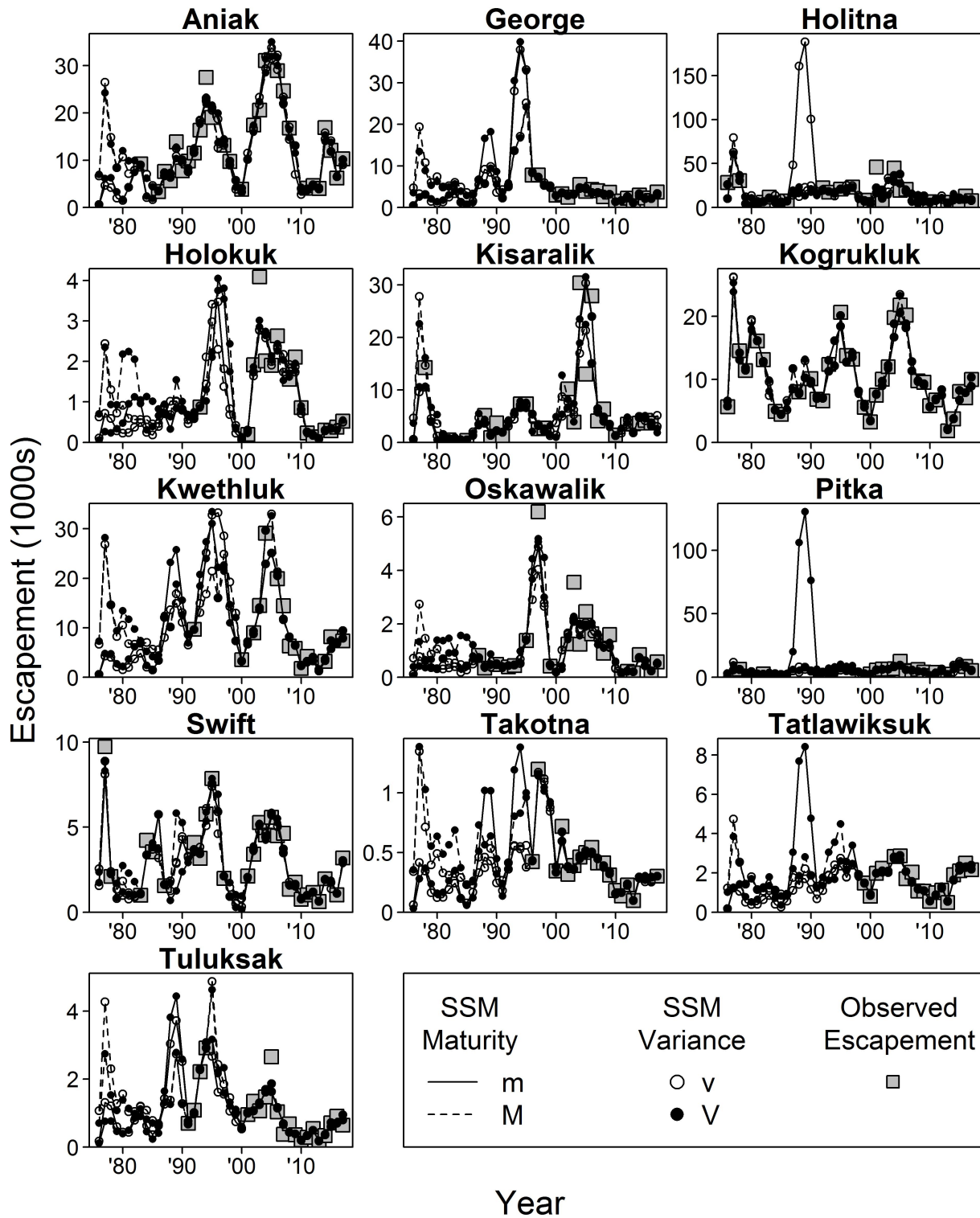


Figure 1.3: Observed and fitted escapement time series for each Kuskokwim River substock. Line/symbol types denote the particular state-space model and grey squares denote observed data.

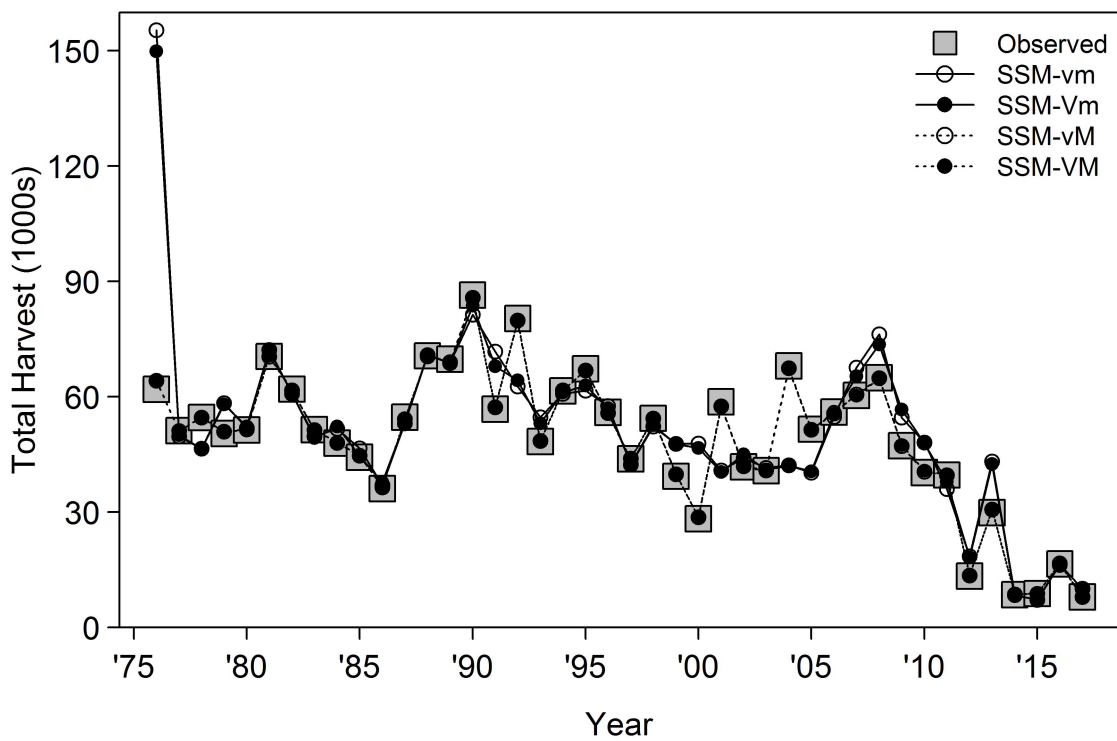


Figure 1.4: Observed and fitted harvest time series aggregated across all Kuskokwim River substocks included in this analysis. Line/symbol types denote the particular state-space model and grey squares denote observed data.

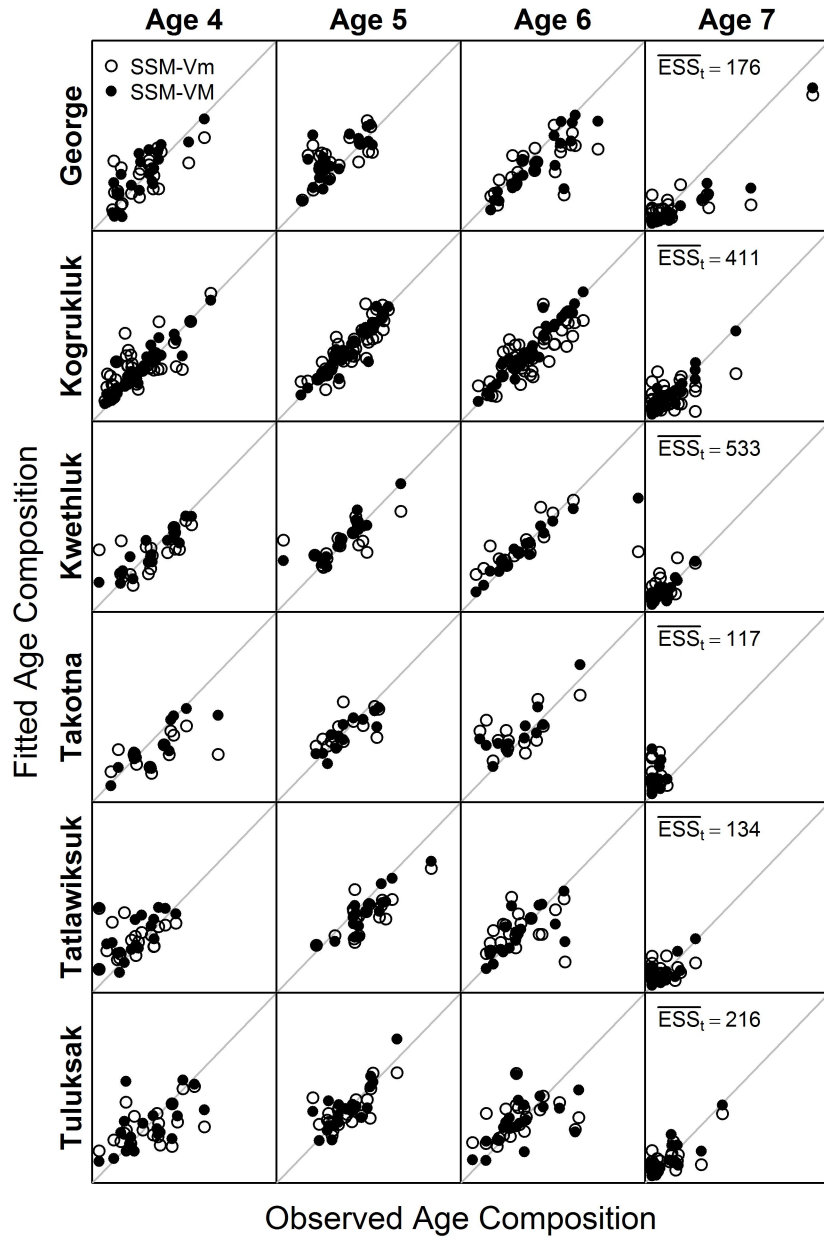


Figure 1.5: Observed and fitted age composition for the 6 weir-monitored substocks. Each scatter plot is the pair of fitted *versus* observed proportion of the escapement in each age each year with data available and the grey line represents the 1:1 perfect fit line. Point types denote two models: SSM-Vm (time-constant maturity; hollow circles) and SSM-VM (time-varying maturity; filled circles). \overline{ESS}_t represents the average number of fish successfully aged each year with data for each substock, which was used as the sample size to weight the data in the multinomial likelihoods that used these data. Panels are scaled to have the same *x*-axis and *y*-axis limits within an age across substocks and range from 0 – 1 for ages 4 – 6 and 0 – 0.3 for age 7.

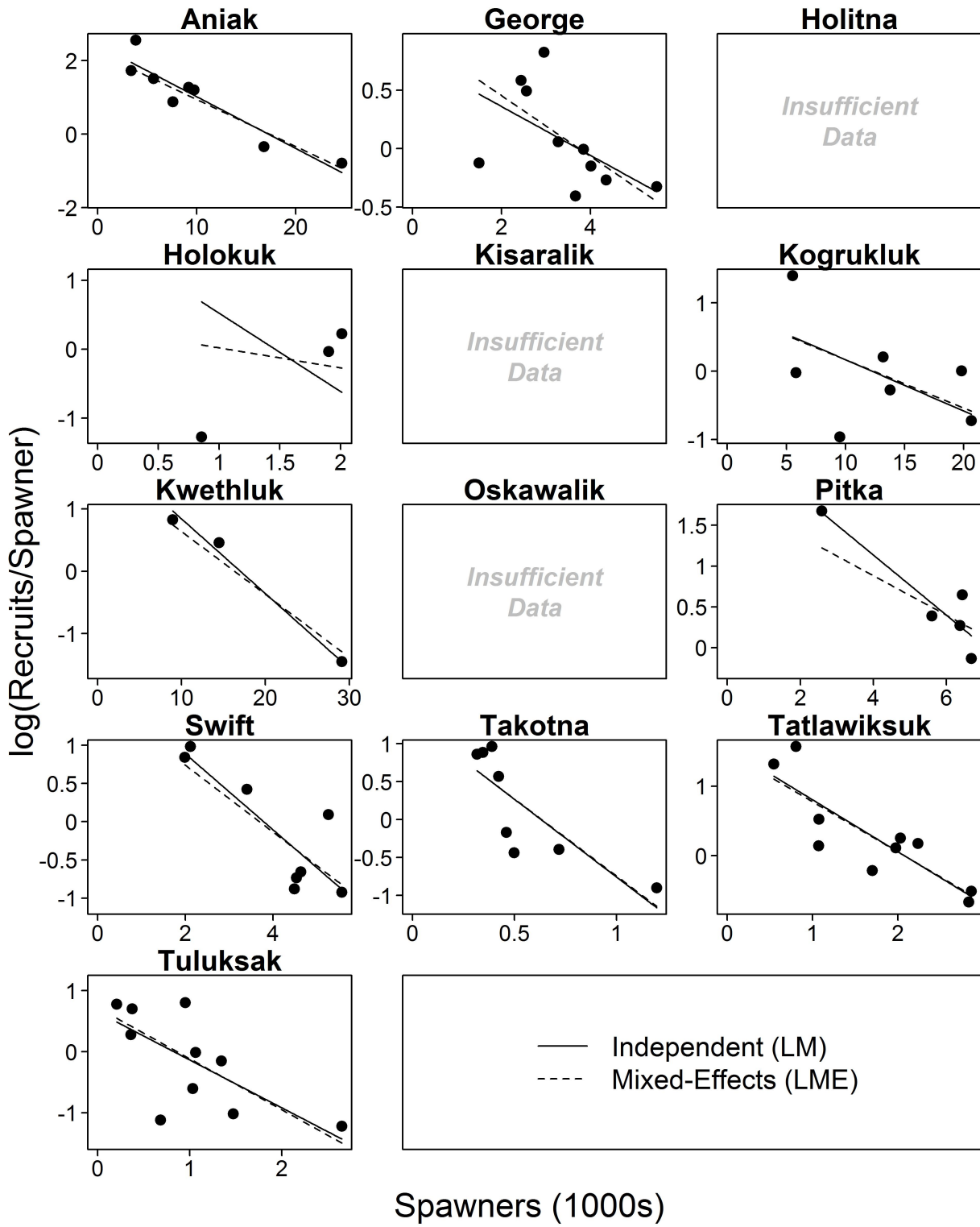


Figure 1.6: Fit of the regression approaches to fitting the multi-stock spawner-recruit analysis to the Kuskokwim River substock data. Points are observed $\log(\text{recruits/spawner})$ versus spawners, solid lines represent the fit for the independent regression models, and dashed lines represent the fit suggested by the model with random intercept effects for each substocks. Three substocks had fewer than 3 observed data points, rendering fitting a regression line infeasible. Note that a constraint was imposed that maintained $\log(\alpha_j) > 0$ which prevented biologically implausible values, and explains the poor fit for the Holokuk River substock.

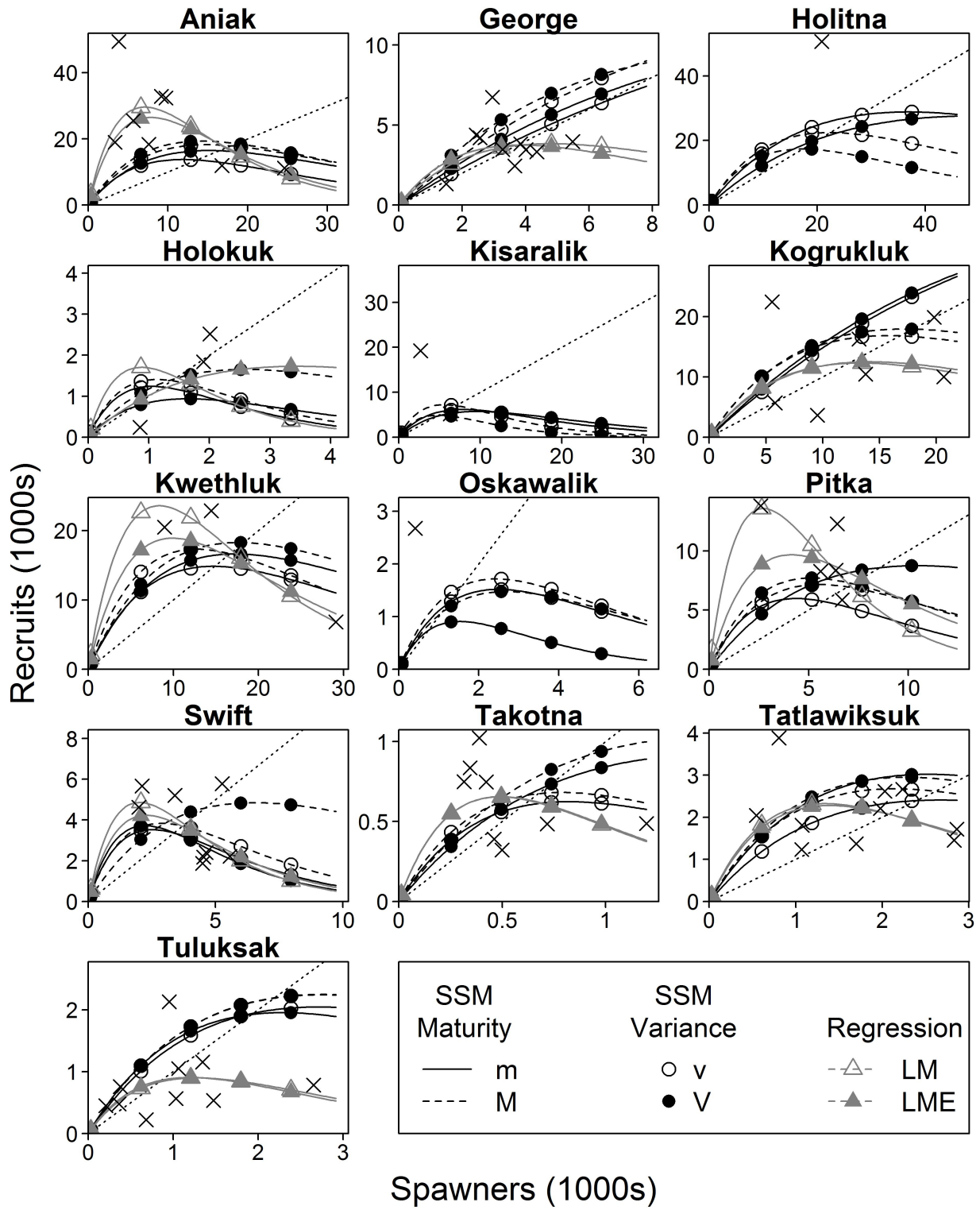


Figure 1.7: Fitted spawner-recruit relationships for the 13 substocks monitored in the Kuskokwim River subdrainage included in this analysis. Line and point types correspond to different models; crosses are completely-observed spawner-recruit pairs. Note that the regression approaches (grey lines/triangles) fitted only to these data, the state-space models (black lines/circles) fitted to all observations of substock-specific escapement, aggregate harvest, and age composition.

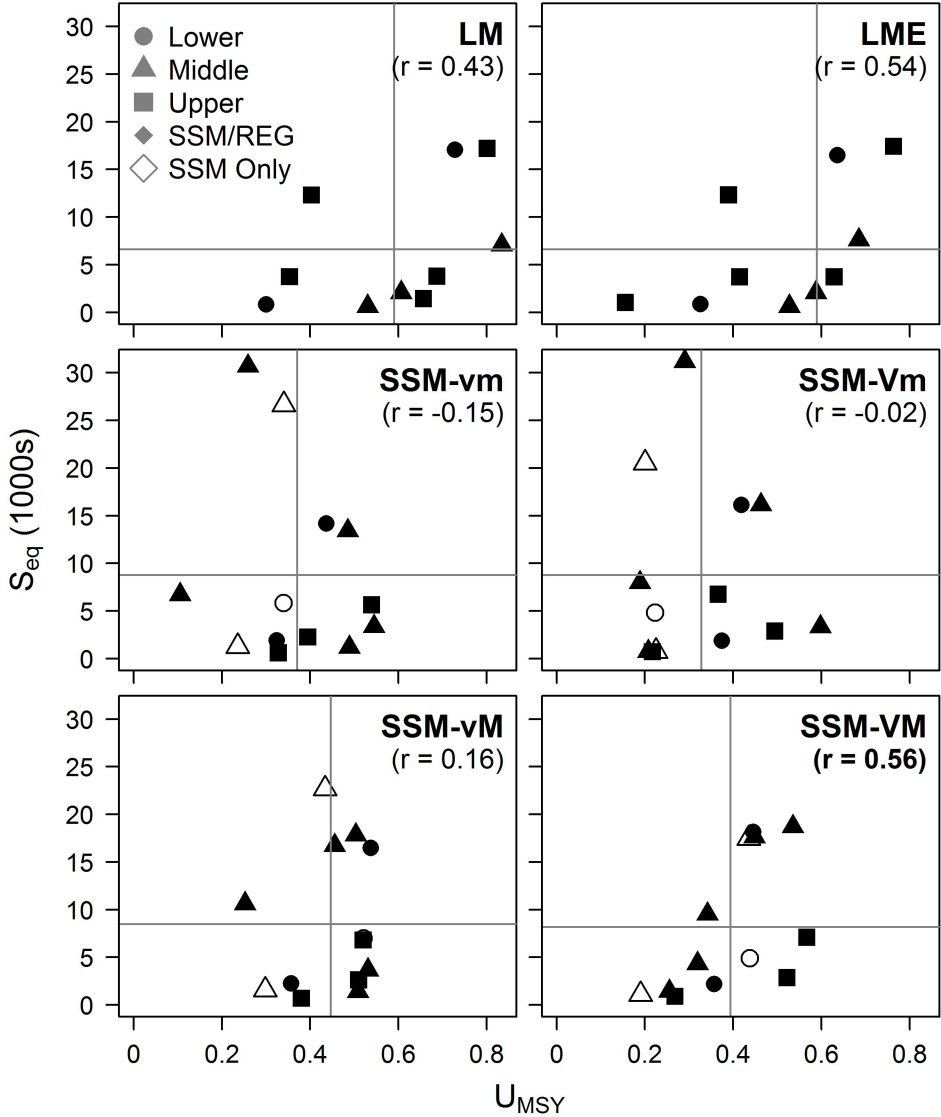


Figure 1.8: Relationships between substock size and productivity as estimated by the 6 estimation approaches in the analysis. Symbol shapes denote the region within the Kuskokwim drainage the substock is located in and hollow symbols in the state-space models are substocks that could not be fitted by the regression approaches. The value in parentheses is Pearson's r correlation coefficient; bold numbers indicate a significant correlation at $\alpha = 0.05$.

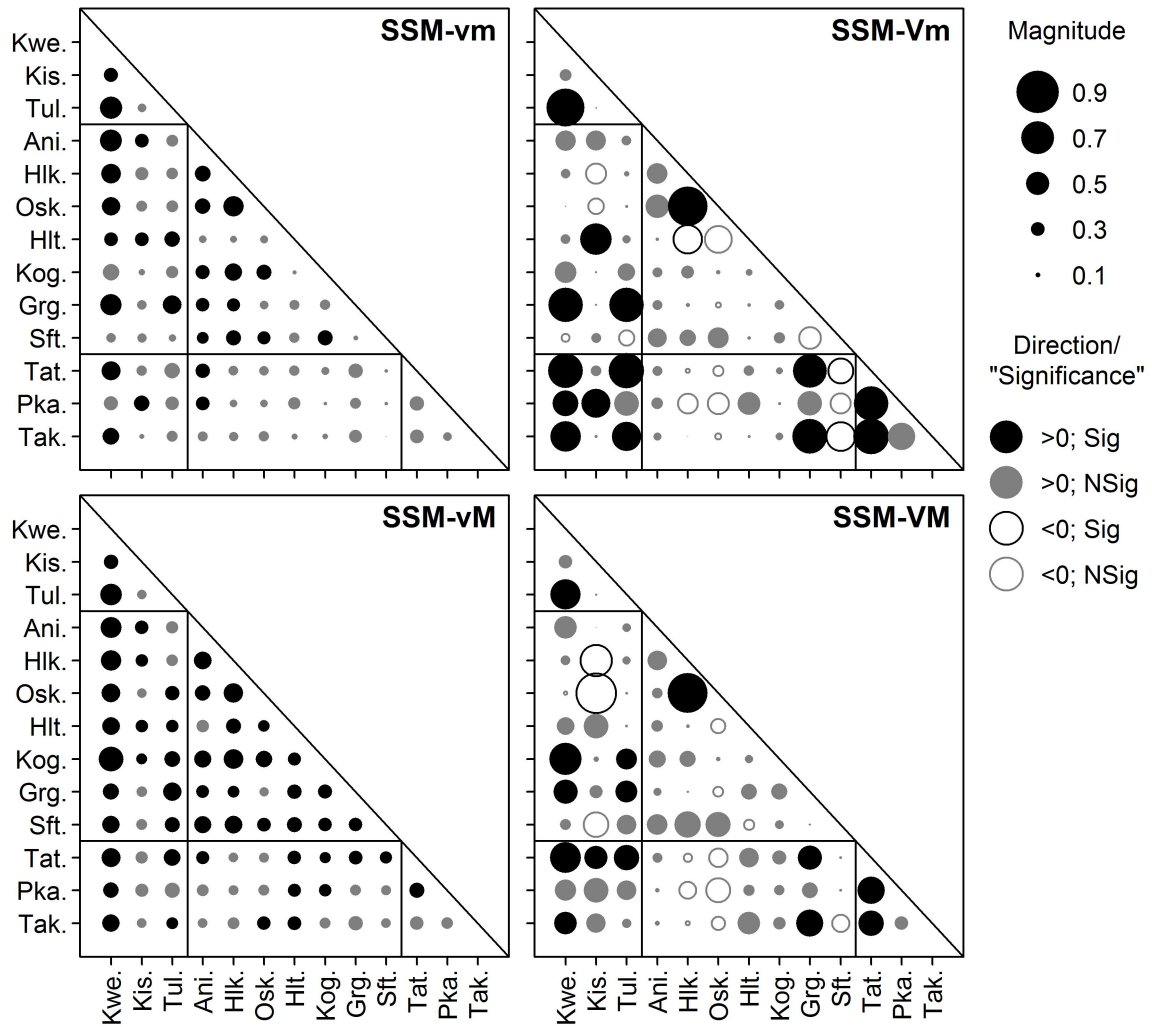


Figure 1.9: Correlation coefficients between recruitment residuals for each substock-pair. The size of each circle represents the magnitude of the correlation, color represents significance (whether 95% credible interval includes 0), and fill represents directionality as described in the legend. Substocks are ordered from downriver to upriver on both axes, and vertical/horizontal lines denote the boundaries between lower, middle, and upper river substocks.

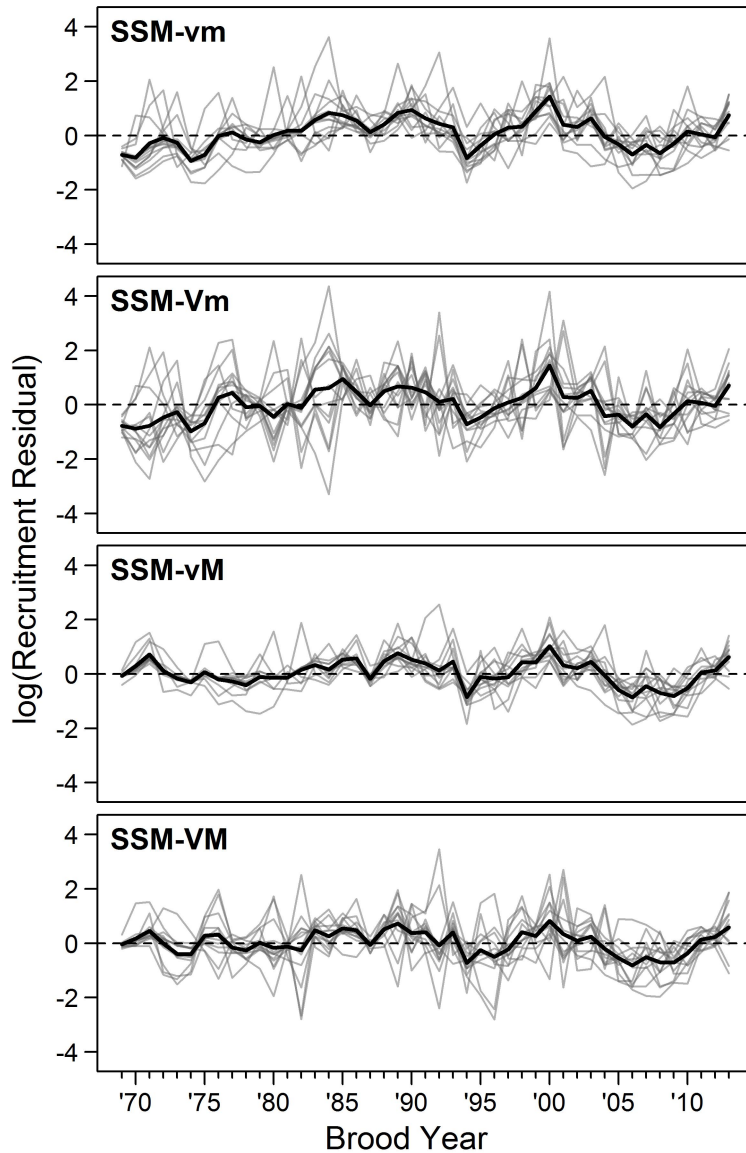


Figure 1.10: Time series of recruitment residuals for each substock under each of the four state-space models. Substock-specific time series are represented by grey lines and the average across substocks within a brood year are represented by the thick black line. A dashed line at zero (no error) is provided for reference.

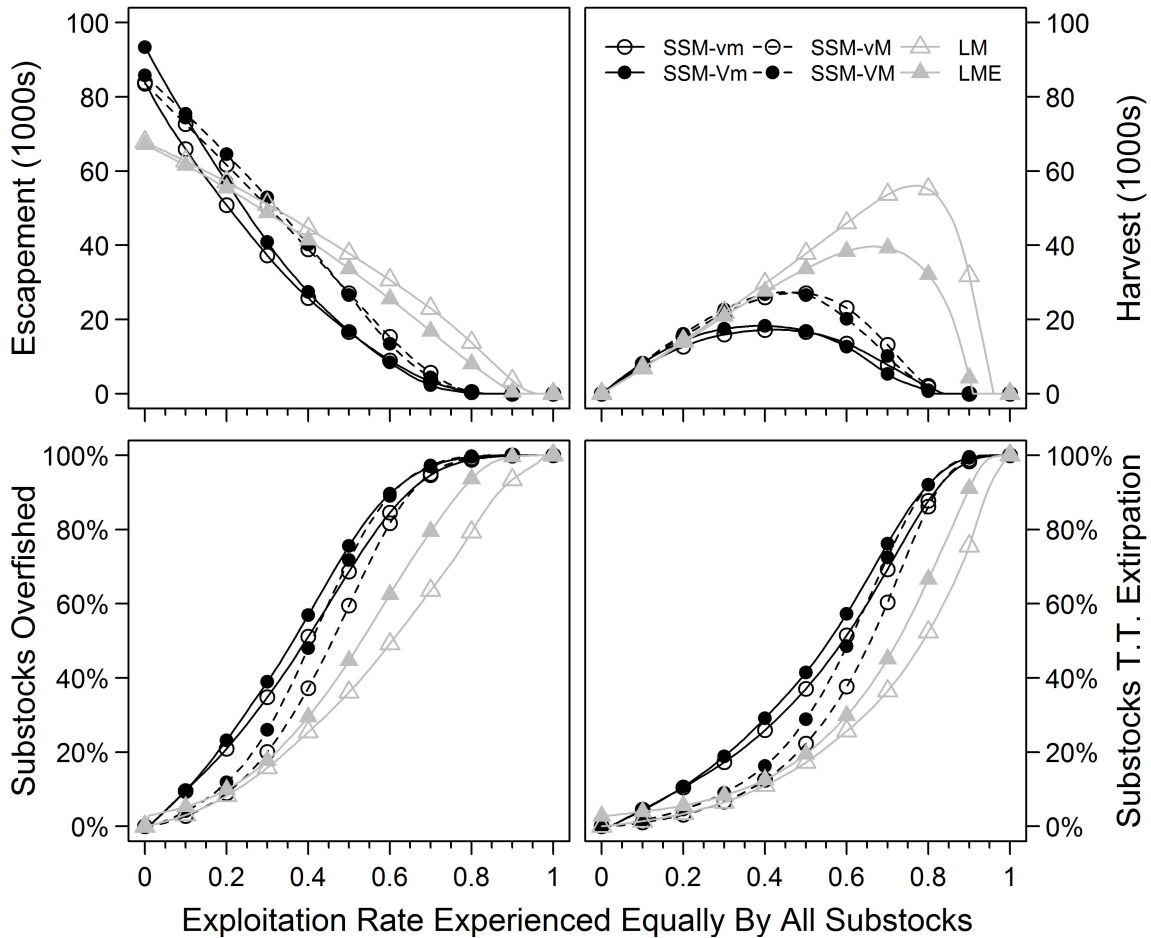


Figure 1.11: Visualization of harvest-biodiversity trade-offs based on equilibrium states (escapement and harvest) of the aggregate stock and the percentage of substocks expected to be in an undesirable state as a function of the exploitation rate under the assumption that all substocks are fished at the same rate. Overfished is defined here as $U > U_{MSY,j}$. “T.T.” stands for “trending toward”, and represents the case where equilibrium escapement would be ≤ 0 . To facilitate comparisons with the regression approaches (grey lines/triangles), the 3 substocks with insufficient data for fitting regression models were excluded from summaries of the state-space models (black triangles/circles).

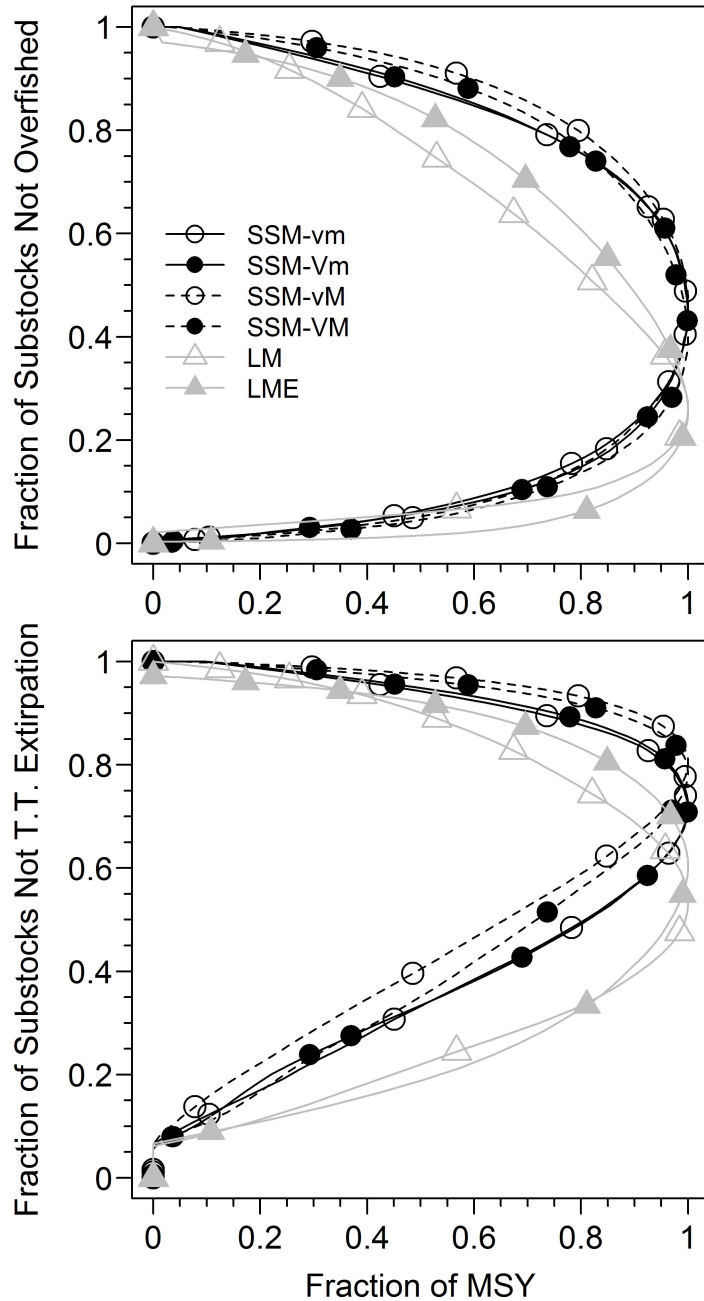


Figure 1.12: Alternative (and more direct than Figure 1.11) visualization of harvest-biodiversity trade-offs for monitored Kuskokwim River Chinook salmon substocks. The conditions of overfished and trending towards extinction are the same as defined in Figure 1.11. These figures should be interpreted by determining how the value of the biodiversity objective (y -axis; expressed as the fraction of substocks that would not be in the undesirable condition) must be reduced to increase the value of the harvest objective (y -axis; expressed as a fraction of the maximum sustainable yield). To facilitate comparisons with the regression approaches (grey lines/triangles), the 3 substocks with insufficient data for fitting regression models were excluded from summaries of the state-space models (black triangles/circles). All symbols represent increasing exploitation rates in increments of 0.1 as you move down the y -axis.

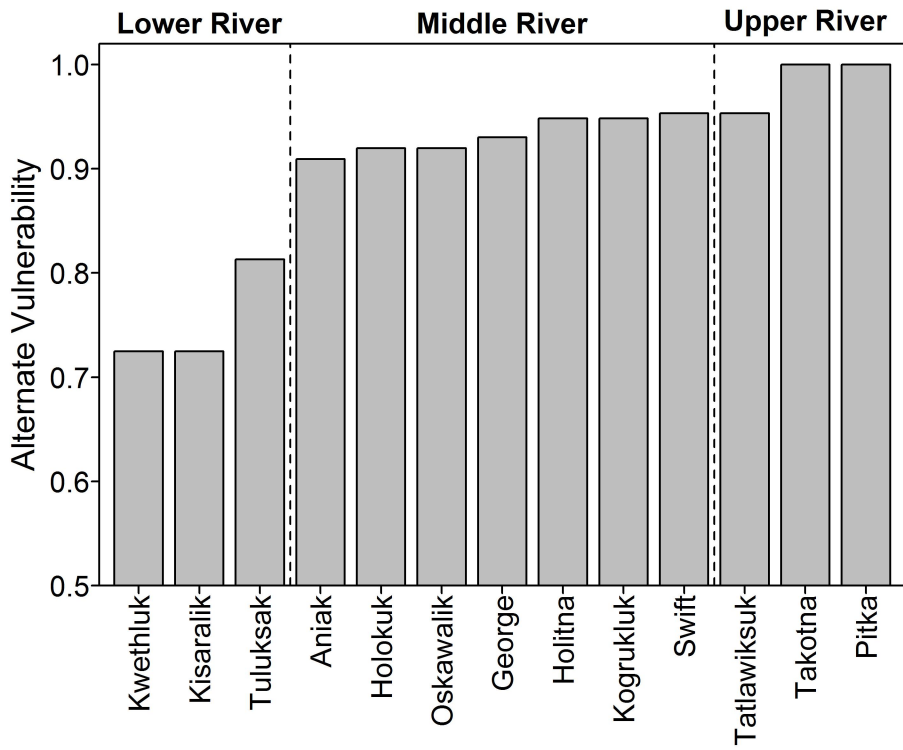


Figure 1.13: Alternative vulnerability schedule (v_j) used in a sensitivity analysis of the state-space models. Vulnerabilities were obtained by determining the fraction of total fishing households the individual substocks must swim past in order to reach their respective natal spawning grounds. Substocks are ordered from downstream to upstream.

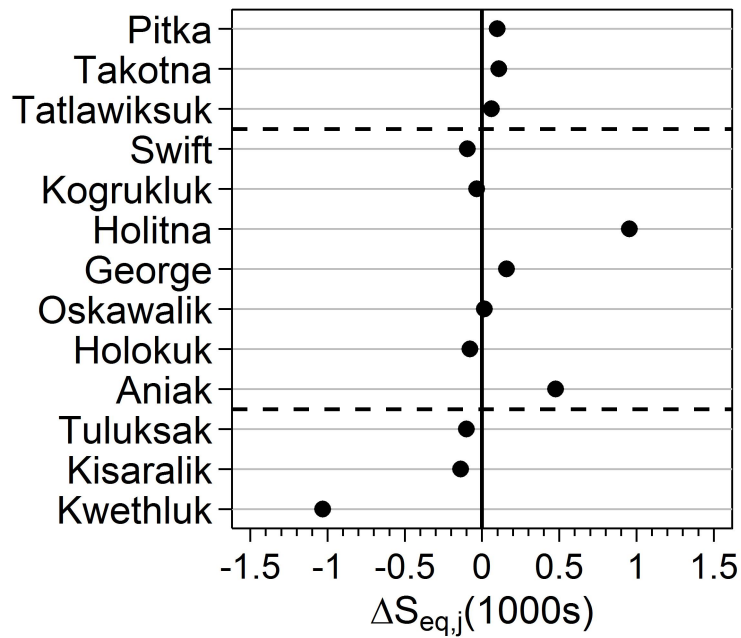
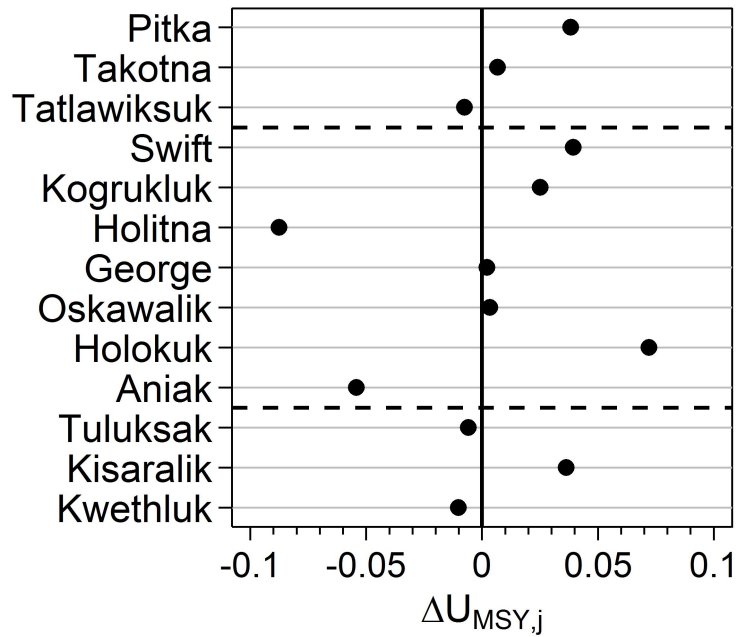


Figure 1.14: Difference in substock-specific parameter estimates between the alternative and default vulnerability schedules. Positive differences indicate that the alternative estimates were larger than the default estimates. Estimates are displayed for SSM-VM only, all other state-space models returned similar differences.

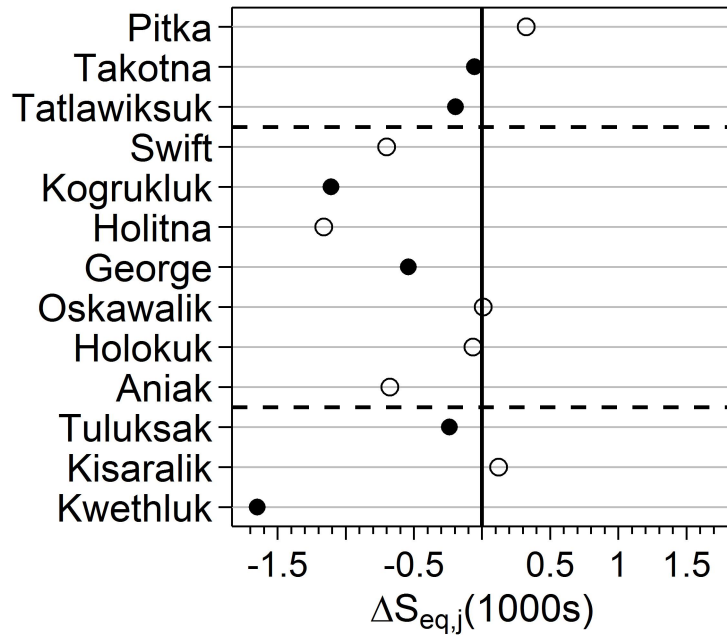
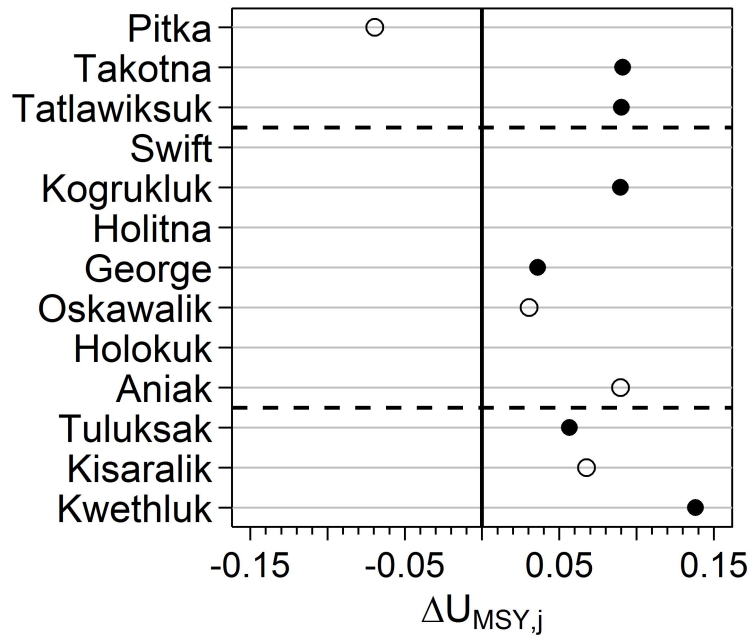


Figure 1.15: Difference in substock-specific parameter estimates between the alternative and default age composition weighting schemes. Positive differences indicate that the alternative estimates were larger than the default estimates. Filled symbols denote substocks with age composition data. Estimates are displayed for SSM-VM only, all other state-space models returned similar differences.

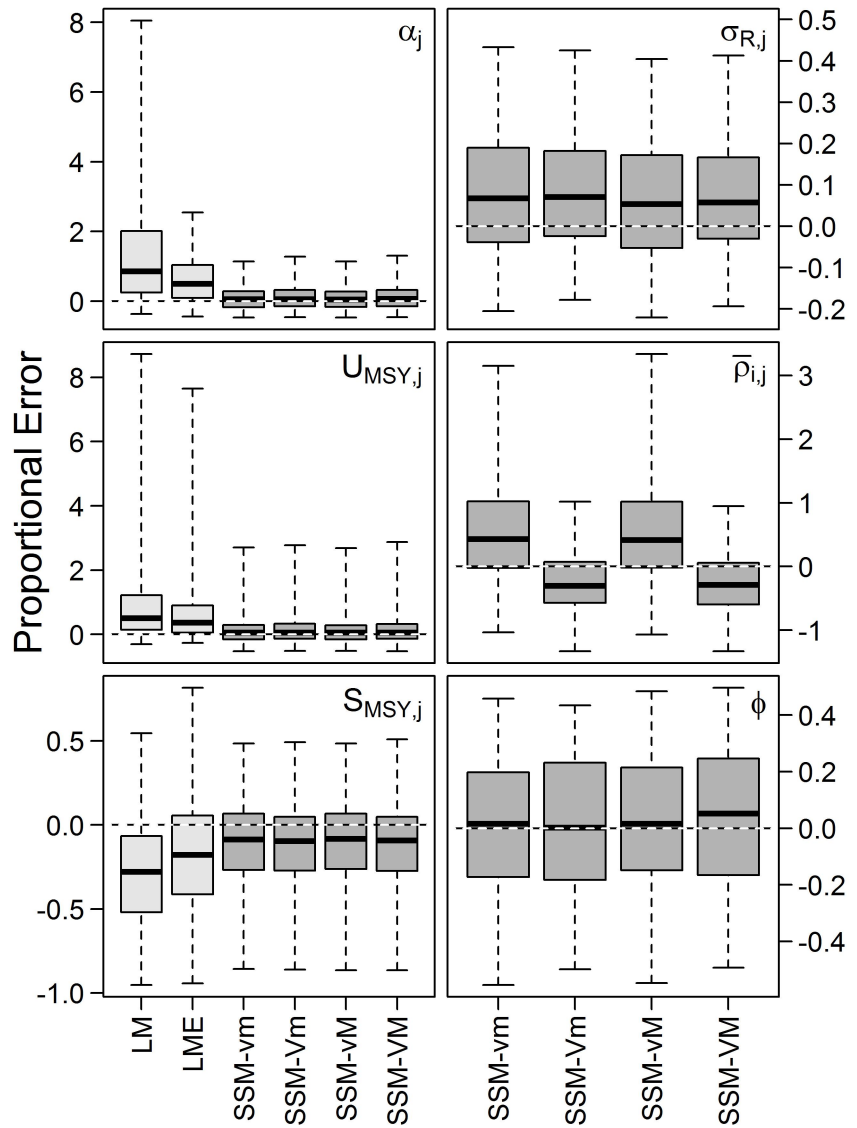


Figure 1.16: Central tendency and variability in proportional error for some parameters in the multi-stock spawner-recruit models from the simulation-estimation trials. Point estimates used were posterior medians.

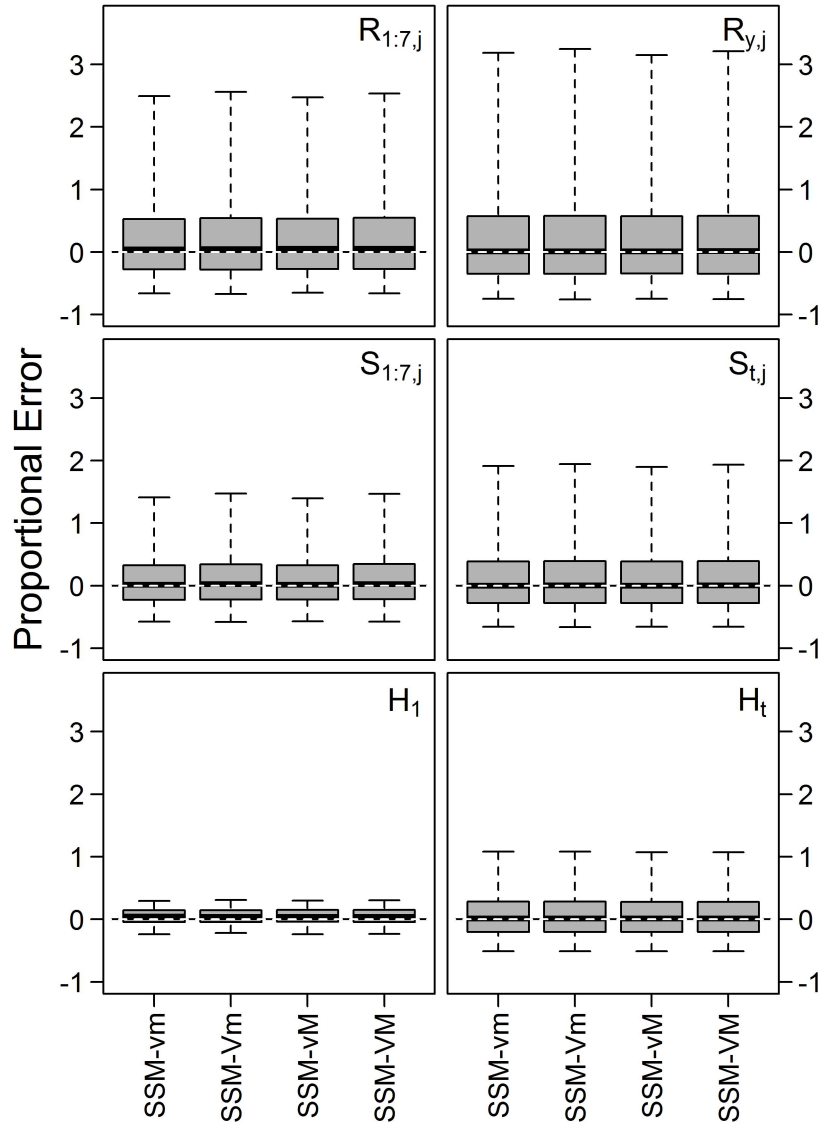


Figure 1.17: Central tendency and variability in proportional error for some abundance states in the multi-stock spawner-recruit models from the simulation-estimation trials. Quantities are separated by the early portion of the time series (left panels) and the entire time series (right panels). Point estimates used were posterior medians.

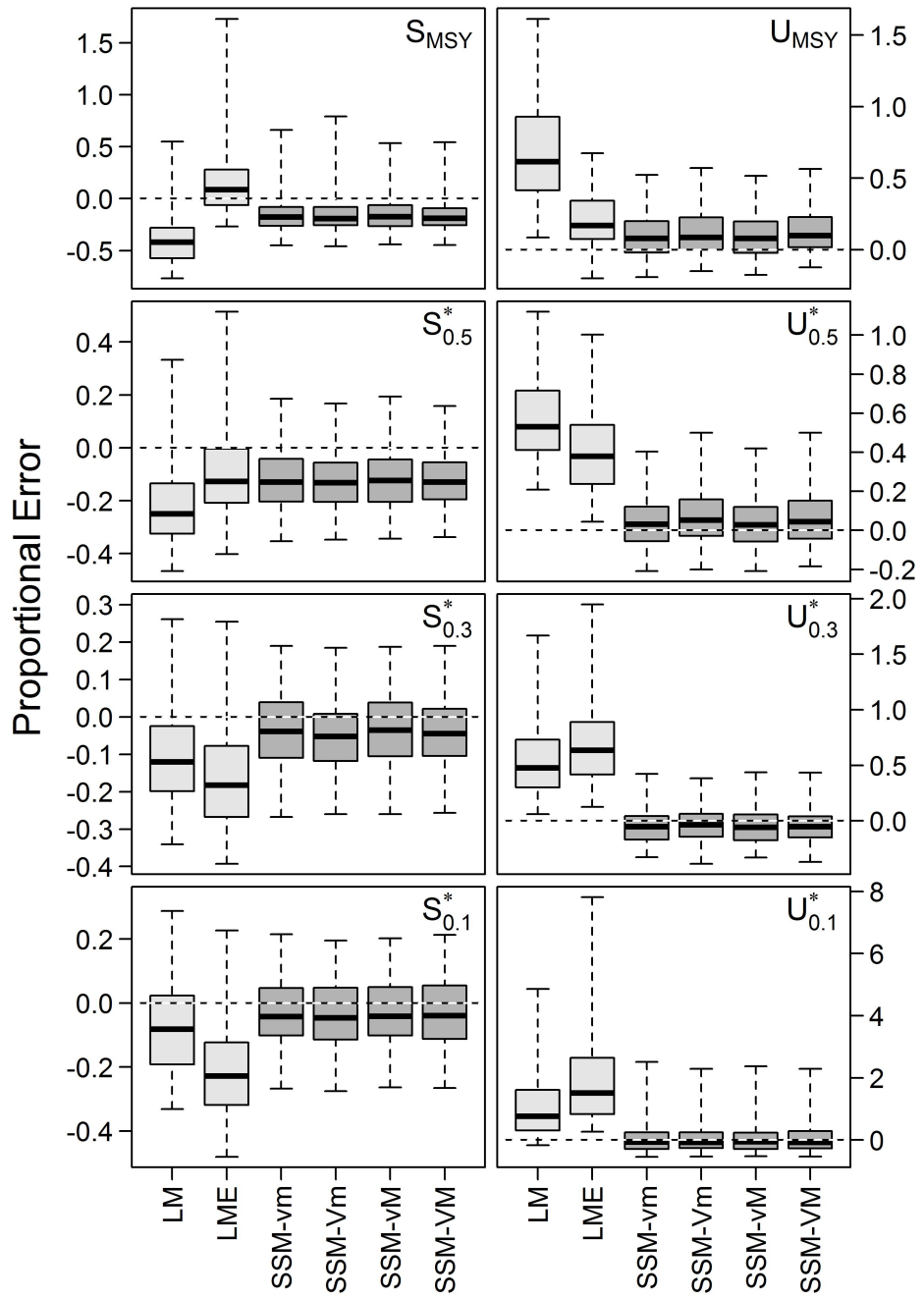


Figure 1.18: Central tendency and variability in proportional error for key biological reference points of the aggregate mixed stock. S_p^* and U_p^* are the aggregate escapement and fully-vulnerable exploitation rate that would ensure no more than $p \cdot 100\%$ of substocks are overfished, respectively. Point estimates used were posterior medians.

Appendix A

Preparation of Data for Fitting Spawner-Recruit Models to Substocks of Kuskokwim River Chinook Salmon in Chapter 1

A.1 Overview of data needs

All data for this analysis are available to the public, and came primarily from the Arctic-Yukon-Kuskokwim Database Management System (AYKDBMS)¹ maintained by the Alaska Department of Fish and Game (ADF&G). Cases in which other data sources were necessary are highlighted in the description below, e.g., the telemetry data needed to perform the expansion of aerial survey counts described in Section A.2 below.

This analysis required three primary data sources:

- (1) Estimates of annual escapement to each of the substocks included.
- (2) Estimates of annual harvest. Linear regression models (Section 1.2.1.1) required harvest apportioned to each substock, the state-space models (Section 1.2.1.2) required only total aggregate harvest summed across all substocks included.
- (3) Estimates of annual age composition (i.e., the fraction of the run each year made up of each age) for all substocks that have had it collected.

Any of these data sources could have missing years.

¹<http://www.adfg.alaska.gov/CommFishR3/WebSite/AYKDBMSWebsite/Default.aspx>

A.2 Substock escapement

Escapement count data for this analysis were informed predominately by the ADF&G Kuskokwim River salmon escapement monitoring program, the details of which have been most-recently documented in Head and Liller (2017). The data set available spans 20 different escapement monitoring projects (6 weirs and 14 aerial surveys) and 42 calendar years from 1976 – 2017. For substocks monitored *via* weir, observed substock j escapement in year t ($S_{obs,t,j}$) was taken to be the total estimated weir passage each year. Substocks monitored *via* aerial survey needed special care, however. Surveys have been flown only once per year on a relatively small fraction of each tributary system (Head and Liller 2017), resulting in these data being indices of escapement rather than estimates of total escapement. This analysis required estimates of total escapement to each substock however, because this would allow calculation of biological reference points that are expressed in terms of the scale of the population (e.g., the spawner abundance that is expected to produce maximum recruitment; $S_{MAX,j}$), rather than as a rate (i.e., $U_{MSY,j}$). Note that if only estimates of $U_{MSY,j}$ were desired, no accounting for the partial counts would be necessary.

The approach I developed to estimate total escapement from single-pass aerial surveys involved two main steps:

- (1) Mapping the distribution of detected telemetry-tagged Chinook salmon against distribution of the aerial survey counts. This comparison allowed for a spatial expansion to estimate how many salmon would have been counted had the entire tributary been flown.
- (2) Obtaining and applying a temporal correction factor for the problem of counting a dynamic pool at one point in its trajectory. This correction factor was based on the relationship between paired weir and aerial counts on $n = 3$ of the systems in the analysis.

A.2.1 Spatial expansion

The core of the spatial expansion estimator was the assumption:

$$\frac{A_{f,t,i}}{T_{f,t,i}} = \frac{A_{u,t,i}}{T_{u,t,i}}, \quad (\text{A.1})$$

where the quantities A and T represent fish and tags, respectively in flown (A_f and T_f) and unflown (A_u and T_u) reaches in year t and for aerial survey monitoring project i . This assumption states that the ratio of spawners per one tagged spawner is the same between flown and unflown river sections at the time of the aerial index count and the aerial telemetry flights. Equation (A.1) can be rearranged as:

$$A_{u,t,i} = A_{f,t,i} \frac{T_{u,t,i}}{T_{f,t,i}}. \quad (\text{A.2})$$

If $T_{u,t,i}$ is further assumed to be a binomial random variable with time-constant success parameter p_i , then:

$$T_{u,t,i} \sim \text{Binomial}(p_i, T_{u,t,i} + T_{f,t,i}). \quad (\text{A.3})$$

Here, p_i represents the probability that a tagged fish in the spawning tributary monitored by project i was outside of the survey flight reach at the time of the aerial telemetry flight. When (A.3) is rearranged to put p_i on the odds scale, then:

$$\psi_i = \frac{p_i}{1 - p_i}. \quad (\text{A.4})$$

Estimated expansion factors ψ_i and p_i are shown in Table A.1. The odds value ψ_i can be substituted for the division term in (A.2) which gives:

$$A_{u,t,i} = A_{f,t,i}\psi_i. \quad (\text{A.5})$$

To obtain the total number of fish that would have been counted had the entire subdrainage been flown ($\hat{A}_{t,i}$), the components can be summed:

$$\hat{A}_{t,i} = A_{f,t,i} + A_{u,t,i}. \quad (\text{A.6})$$

Substitution of (A.5) into (A.6) and factoring gives the estimator:

$$\hat{A}_{t,i} = A_{f,t,i}(1 + \psi_i). \quad (\text{A.7})$$

The spatial expansion model was integrated with the temporal expansion model described below into a single model fitted in the Bayesian framework fitted using JAGS (Plummer 2017). This allowed for seamless propagation of uncertainty (in ψ_i) from the expansion above to the next step.

A.2.2 Temporal Expansion

The temporal expansion model was necessary to convert from the one-pass index scale to the substock total annual escapement scale: it was a temporal correction. The temporal expansion I developed operated by first regressing $n = 16$ observations of paired weir count (W_i) and spatially-expanded aerial counts (\hat{A}_i ; given by (A.7)) on the same tributary systems ($n = 3$) in the same years:

$$W_i = \beta_0 + \beta_1 \hat{A}_i + \varepsilon_i, \quad (A.8)$$

$$\varepsilon_i \stackrel{\text{iid}}{\sim} N(0, \sigma_W)$$

The estimated coefficients $\hat{\beta}_0$ and $\hat{\beta}_1$ (Table A.2) were then applied to tributary systems with an aerial count but not a weir count:

$$S_{obs,t,j} = \hat{\beta}_0 + \hat{\beta}_1 \hat{A}_{t,j} \quad (A.9)$$

The fitted relationship is shown in Figure A.2. For substocks that had both weirs and aerial surveys, the weir count was used as $S_{obs,t,j}$ as opposed to using the expansion in (A.9) and the coefficient of variation (CV) representing observation uncertainty for the state-space models (Section ??) was set at 5%, which assumed annual escapement counts made at weirs are precise. For substocks monitored solely *via* aerial survey, the posterior mean value of $S_{obs,t,j}$ was used as the escapement count that year, and the posterior CV was calculated for use as the observation uncertainty passed to the state-space models.

A.3 Aggregate harvest

Harvest estimates for the Kuskokwim River are available at the drainage-wide scale only, and were obtained each year by subtracting the drainage-wide estimates of total run and escapement (Liller et al. 2018). Because the escapement data used here do not encompass all the substocks within the Kuskokwim River system, it was necessary to remove some portion of the total harvest that was produced by stocks not included in this analysis. First, I calculated the observed exploitation rate of the drainage-wide Kuskokwim River Chinook salmon stock ($U_{obs,t}$) by dividing the total harvest by the total run each year. I then made the

assumption that monitored and unmonitored substocks have received the same exploitation rates, in which case total harvest accounted for in this analysis harvest was obtained as:

$$H_{obs,t} = \frac{S_{obs,t} U_{obs,t}}{1 - U_{obs,t}}, \quad (\text{A.10})$$

which can be derived from the definition of the exploitation rate ($U = \frac{H}{S+H}$). This step was embedded within the same Bayesian model that encompassed the spatial and temporal aerial survey expansions such that uncertainty in these steps could be propagated through the entire analysis. The posterior mean value of $H_{obs,t}$ was used as the observed total harvest data, and the posterior CV was retained for use as the observation error attributed to this data source.

Note that $S_{obs,t}$ and $H_{obs,t}$ do not have j subscripts denoting particular substocks: this indicates that they are aggregate quantities summed across all substock components. In cases where substock-specific harvest was desired (i.e., in reconstructing the substock-specific brood tables for fitting individual regression relationships; Section A.5), $H_{obs,t,j}$ was obtained using (A.10) by substituting $S_{obs,t,j}$ in for $S_{obs,t}$.

A.4 Age composition

Age composition data were necessary to reconstruct brood tables for age-structured salmon populations (see Section A.5). Age data used in this analysis came from the ADF&G standardized age, sex, and length sampling program operated at the weir projects. All sampled fish that were not aged successfully were discarded as were samples corresponding to the rare ages of 3 and 8 such that only fish successfully aged as between 4 and 7 were included. It is possible that older or younger fish may have the systematic tendency to return early or late in the run, and this could introduce biases if age sampling was not conducted

proportionally to fish passage throughout the season. To adjust for this possibility, a weighted-average scheme was applied to obtain the age composition estimates for each substock and year with data. Daily age samples were stratified into two-week strata and strata-specific proportions-at-age were calculated. These strata-specific age compositions were then averaged across strata within a year and stock weighted by the number of Chinook salmon estimated to have passed the weir in each stratum. The total number of fish successfully aged for each year and substock was retained for data-weighting purposes for the state-space models, which (unlike the regression-based approaches) internally reconstructed the brood tables (see Section ??).

A.5 Brood table reconstruction

An important consideration in the use of the regression-based method is in how $RPS_{y,j}$ is obtained for salmon stocks that return at more than one age (like Chinook salmon). Only the states $S_{y,j}$ are ever directly observed; $R_{y,j}$ is observed (for Chinook salmon) over four calendar years as not all fish mature and make the spawning migration at the same age. Thus, in order to completely observe one $RPS_{y,j}$ outcome, escapement must be monitored in year y and escapement, harvest, and age composition must be monitored in the subsequent years $y + 4$, $y + 5$, $y + 6$, and $y + 7$. It is evident that missing one year of sampling (which is common; Figure A.1) can lead to issues with this approach. Only completely observed $RPS_{y,j}$ data were used for this analysis, with the exception of missing age composition data. For substocks with no age composition data (i.e., those monitored *via* aerial survey), the average age composition each year across substocks that have data was used to reconstruct $RPS_{y,j}$, but was provided only for years with escapement sampling for substock j . Only substocks with ≥ 3 completely-observed pairs of $RPS_{y,j}$ and $S_{y,j}$ were included for model fitting, given each fitted line was dictated by 2 parameters.

A.6 Results

A.6.1 Escapement

The expansion of aerial survey data to obtain total annual escapement estimates (described in Appendix A.2) produced reasonable estimates of both expansion factors and escapement. For the spatial expansion (which used the distribution of telemetry-tagged fish with respect to the aerial survey reaches as described in Appendix A.2.1), the escapement project that received the largest expansion was the Holitna River, with an expansion factor ($1 + \psi_j$) of 4.78 (4.04 – 5.73; 95% equal-tailed credible limits) as shown in Table A.1. Given the small length of surveyed stream relative to the size of the Holitna subdrainage (Figure 1.2; substock #7), this large estimate makes intuitive sense. The aerial survey project that required the smallest spatial expansion was the Salmon fork of the Aniak River (1.04; 1.01 – 1.14; Table A.1). The average spatial expansion factor across all aerial survey projects was 1.78 (1.67 – 1.93).

In terms of the temporal expansion (intended to adjust the aerial counts for their single-pass nature; Appendix A.2.2), the estimate for the primary expansion coefficient ($\hat{\beta}_1$) was 2.3 (1.76 – 2.85; Table A.2). This estimate indicates that spatially-corrected aerial survey counts needed to be scaled up by a factor of 2.3 in order to be consistent with the total annual escapement counts made at weirs in years and subdrainages that had paired counts. This estimate makes intuitive sense given ADF&G has structured the timing of aerial survey flights to coincide with the peak of the escapement timing arrival curve (Head and Liller 2017), which should occur approximately halfway through the run, indicating the aerial counts would need to be doubled to account for the second half of the run. The freely-estimated intercept of the temporal expansion ($\hat{\beta}_0$) had a value of 1.9 (-60.71 – 62.4), indicating that if no fish are counted by an aerial survey, very little escapement actually occurred (Table

A.2). For the substocks monitored *via* aerial survey that required these expansions, the average annual observation CV was estimated to be 18% (it was set at 5% for weir-monitored substock escapement).

Based on the scale of the summed escapement estimates from this analysis relative to the drainage-wide scale (which includes monitored and unmonitored substocks; Liller et al. 2018), approximately half (57%; 47% – 66%) of the Chinook salmon aggregate population is accounted for by the $n_j = 13$ substocks included here (Figure A.3).

A.6.2 Harvest

The average annual exploitation rate used in this analysis was the same as for the aggregate Chinook salmon population: 0.42 with a minimum and maximum value of 0.13 and 0.62 in 2017 and 1988, respectively. The average annual harvest attributable to substocks included in this analysis was nearly 50,000, which is approximately 57% of the historical average harvest from all substocks in the Kuskokwim River. The average annual observation CV was estimated to be 8%.

A.6.3 Age composition

Age composition data were available for 6 substocks included in this analysis (i.e., those monitored *via* weir: George, Kogrukuk, Kwethluk, Takotna, Tatlawiksuk, and Tuluksak; Appendix A.4). The number of years observed per substock depended on the starting year of the project: each year with an escapement count from a weir had associated age data but not all projects have been operating since 1976. The average annual multinomial sample size ($ESS_{t,j}$) varied between substocks (range 117 – 553) and was generally related to the average escapement counted at each project. Across all substocks, the average annual age

composition was 27%, 38%, 33%, and 2% for ages 4, 5, 6, and 7, respectively, though there was a high degree of inter-annual variability.

Table A.1: The estimated spatial expansion factors for the various aerial survey projects described in Section A.2.1. p_i represents the average fraction of telemetry tags that were detected outside of index flight reaches, which was used as the basis for determining the multiplier $(1 + \psi_i)$ needed to correct the aerial count for not flying the entire subdrainage. In cases where multiple projects were flown to count fish within one substock (e.g., the Aniak, see Figure 1.2 substock 4), the expanded project counts were summed to obtain an estimate for the total substock, as indicated by the footnotes.

Aerial Survey	p_i	$1 + \psi_i$
Kisaralik	0.59 (0.42 – 0.75)	2.46 (1.72 – 4.04)
Salmon (Aniak)^a	0.04 (0.01 – 0.12)	1.04 (1.01 – 1.14)
Aniak^a	0.41 (0.37 – 0.47)	1.71 (1.58 – 1.87)
Kipchuk^a	0.09 (0.04 – 0.17)	1.1 (1.04 – 1.21)
Holokuk	0.37 (0.23 – 0.53)	1.59 (1.3 – 2.12)
Oskawalik	0.44 (0.29 – 0.6)	1.79 (1.4 – 2.52)
Holitna	0.79 (0.75 – 0.83)	4.78 (4.04 – 5.73)
Cheeneetnuk^b	0.25 (0.16 – 0.38)	1.34 (1.18 – 1.61)
Gagaryah^b	0.08 (0.02 – 0.19)	1.08 (1.02 – 1.24)
Salmon (Pitka Fork)^c	0.4 (0.3 – 0.5)	1.66 (1.42 – 2.01)
Bear^c	0.05 (0 – 0.22)	1.05 (1 – 1.28)
Upper Pitka Fork^c	0.62 (0.48 – 0.75)	2.62 (1.92 – 4)

Substocks assessed with multiple aerial survey projects

^a Aniak Substock

^b Swift Substock

^c Pitka Substock

Table A.2: The estimated temporal expansion parameters for converting spatially-expanded aerial counts to estimates of subdrainage-wide escapement abundance each year.

Parameter	Estimate
$\hat{\beta}_0$	1.9 (-60.71 – 62.4)
$\hat{\beta}_1$	2.3 (1.76 – 2.85)
$\hat{\sigma_W}$	4992.15 (3376.54 – 7565.08)

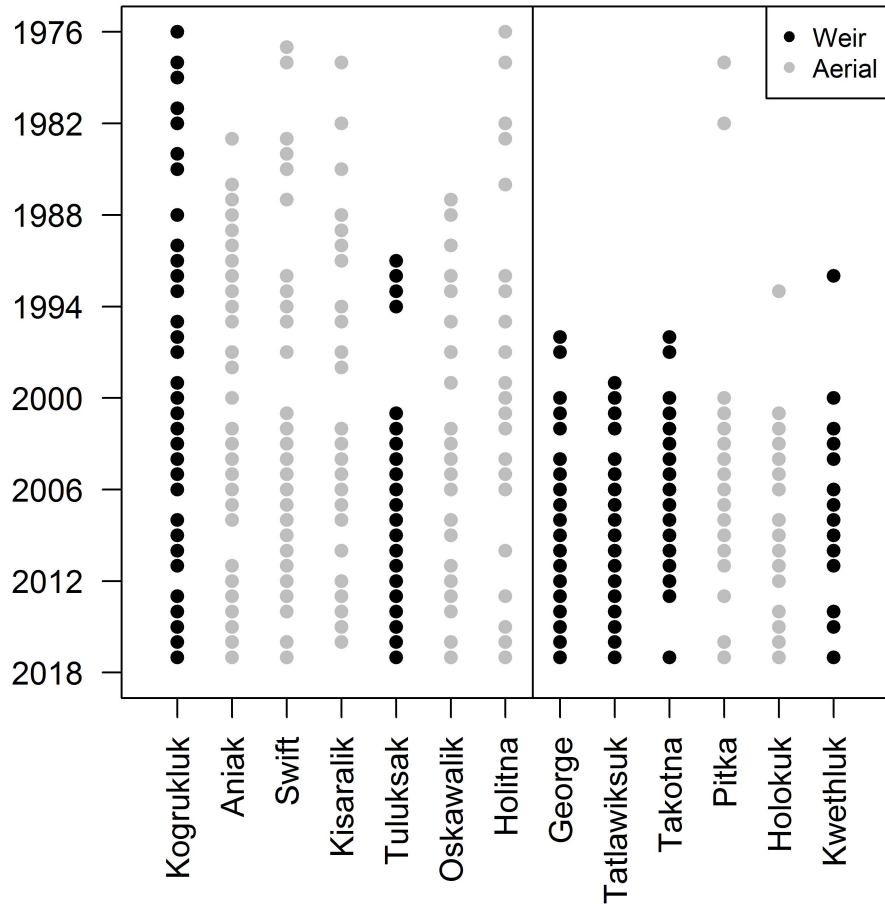


Figure A.1: The frequency of escapement sampling for each substock sampled in the Kuskokwim River. Black points indicate years that were sampled for substocks monitored with a weir and grey points indicate years sampled for substocks monitored with aerial surveys. The vertical black line shows a break where > 50% of the years were monitored for a stock.

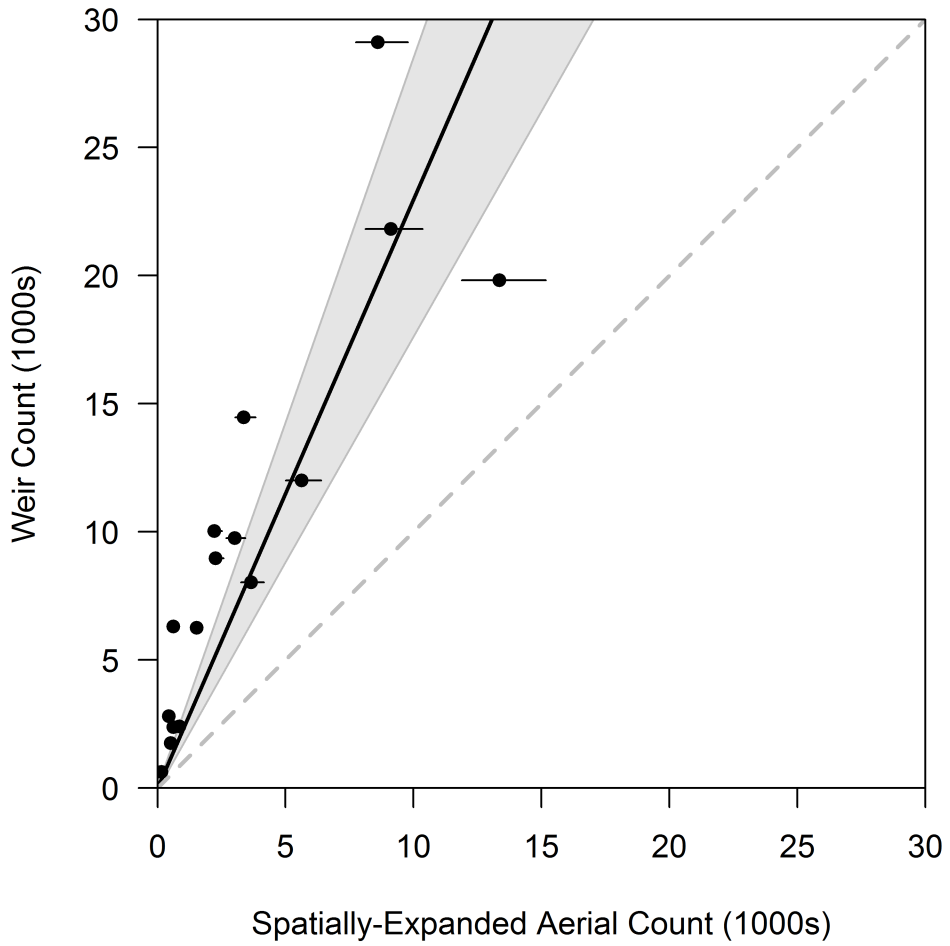


Figure A.2: The relationship between spatially-expanded aerial survey estimates and weir counts during the same years and substocks as described by (A.8). Notice the uncertainty expressed in the predictor variable; this was included in the analysis by incorporating both the spatial (Section A.2.1) and temporal (Section A.2.2) expansions in a single model fitted using Bayesian methods.

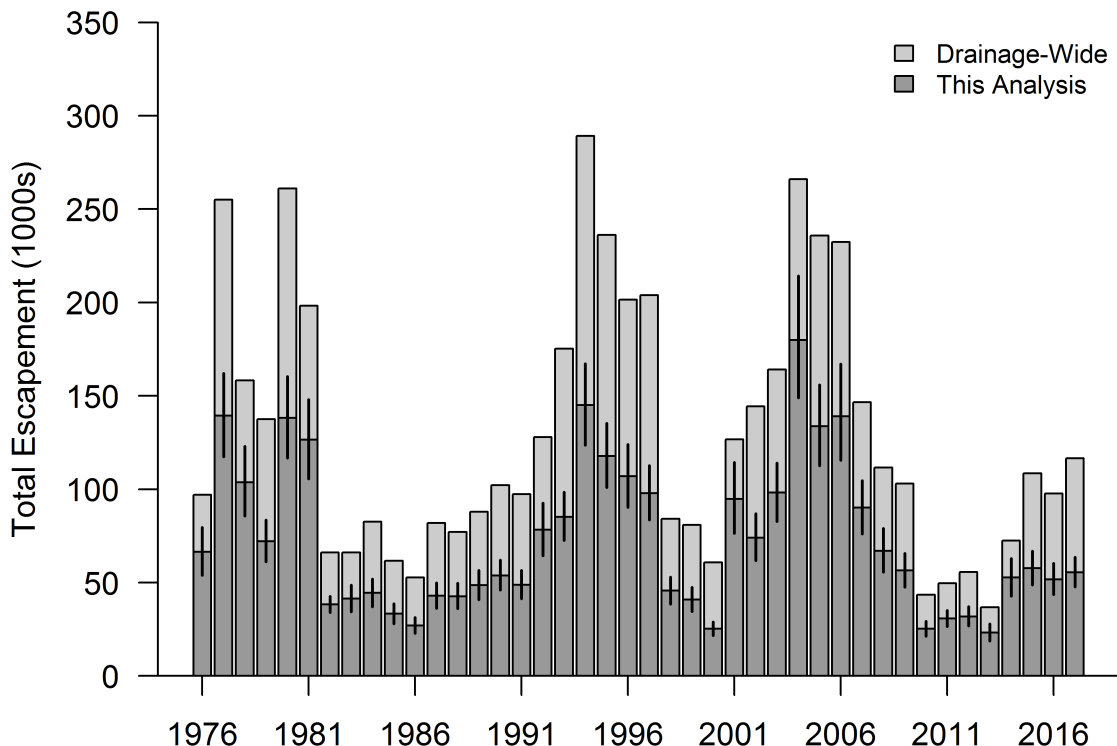


Figure A.3: Estimated Chinook salmon escapement for substocks within the Kuskokwim River drainage. ‘Drainage-wide’ refers to the aggregate population estimates provided by a maximum likelihood run reconstruction model. ‘This analysis’ refers to the estimated portion of the aggregate run included in this analysis (not all tributaries have been monitored).

Appendix B

Simulation of Substock- and Year-Specific Maturity Schedules

In the operating model of the simulation-estimation component of Chapter 1, maturity variability was modeled with more complexity than assumed by the most complex estimation model. It was simulated to vary on average by substock (i.e., some substocks would tend to mature at younger or earlier ages). Additionally, brood-year specific random maturity schedules were generated for each substock, though were simulated to be highly synchronous among substocks. I was unaware of a way to model such correlated dynamics using the Dirichlet random process, so I generated it using a hierarchical linear modeling approach. Note that some of the notation in this appendix uses symbols with different meanings in the main text and other appendices.

B.1 Single substock, single year example

First, define a vector of $n_a - 1$ coefficients:

$$\boldsymbol{\gamma} = \begin{bmatrix} \gamma_0 & \gamma_1 & \gamma_2 \end{bmatrix}$$

and a design matrix with rows and columns equal to $n_a - 1$:

$$\mathbf{X} = \begin{bmatrix} 1 & 0 & 0 \\ 1 & 1 & 0 \\ 1 & 0 & 1 \end{bmatrix}$$

Then, combine them into a linear predictor on the logit scale:

$$\text{logit}(\boldsymbol{\psi}) = \mathbf{X}\boldsymbol{\gamma}$$

The vector $\boldsymbol{\psi}$ contains the probability of maturity at each age, conditional on not having matured at any previous age for the first $n_a - 1$ possible ages-at-maturation. The elements of $\boldsymbol{\psi}$ can be converted to marginal probabilities of maturing at each age (elements of \mathbf{p}):

$$p_a = \begin{cases} \psi_a & \text{if } a = 1 \\ \psi_a(1 - \sum_{a=1}^{a-1} p_a) & \text{if } 1 < a < n_a - 1 \\ 1 - \sum_{a=1}^{n_a} p_a & \text{if } a = n_a \end{cases}$$

These marginal probabilities can be then used to apportion recruitments occurring from brood year y to the various calendar years of observation t .

B.2 Extension to multiple substocks and years

Alterations were made to the γ_0 parameter to be specific to each substock and year combination. Stock-level effects were randomly sampled:

$$\varepsilon_j \sim N(0, \sigma_j),$$

then brood year- and substock-specific random effects were sampled:

$$\varepsilon_{y,1:n_j} \sim \text{MVN}(\varepsilon_{1:n_j}, \Sigma_y),$$

to obtain the year- and substock-specific parameter:

$$\gamma_{0,y,j} = \gamma_0 + \varepsilon_{y,j}.$$

The following parameter values were used: $\gamma_0 = -1.4$, $\gamma_1 = 1.4$, $\gamma_2 = 4$, and $\sigma_j = 0.25$. The covariance matrix Σ_y was constructed with standard deviations for each substock equal to 0.2 and correlation equal to 0.9. These settings resulted in an average vector maturation probabilities of 0.2, 0.4, 0.37, and 0.03 for ages 4, 5, 6, and 7, respectively. An example is shown in Figure B.1.

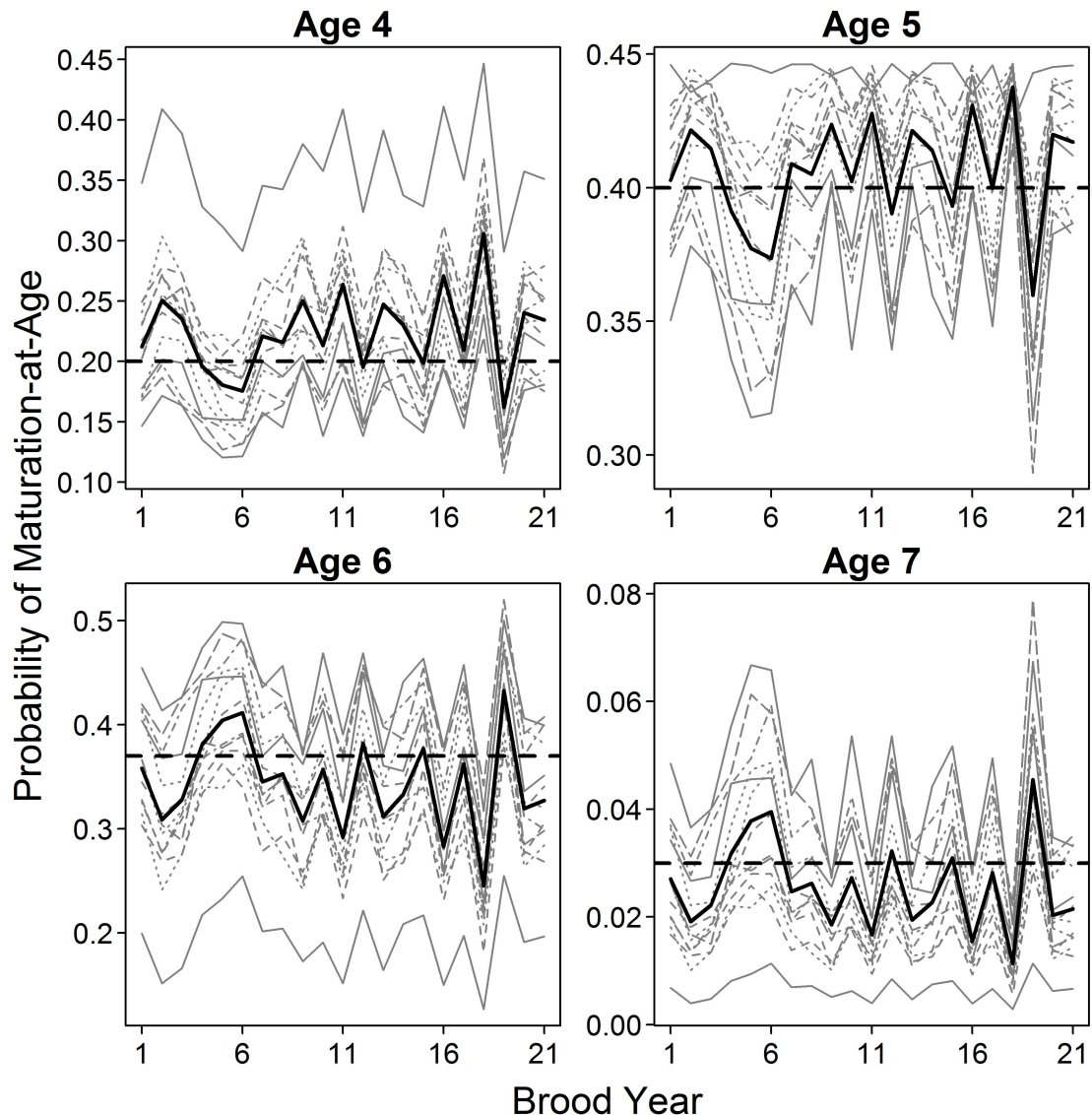


Figure B.1: Simulated probability of maturation-at-age for 13 simulated substocks over time. Note the highly correlated patterns in year-specific variability.

Bibliography

- Blair, G. R., Rogers, D. E., and Quinn, T. P. 1993. Variation in life history characteristics and morphology of sockeye salmon in the Kvichak River system, Bristol Bay, Alaska. *Transactions of the American Fisheries Society*, 122.
- Brooks, S. P. and Gelman, A. 1998. General methods for monitoring convergence of iterative simulations. *Journal of Computational and Graphical Statistics*, 7(4):434.
- Clark, R. A., Bernard, D. R., and Fleischman, S. J. 2009. Stock-recruitment analysis for escapement goal development: A case study of Pacific salmon in Alaska. In Krueger, C. C. and Zimmerman, C. E., editors, *Pacific Salmon: Ecology and Management of Western Alaska's Populations*, American Fisheries Society Symposium 70, pages 743–757, Bethesda, MD.
- Clark, S. C., Tanner, T. L., Sethi, S. A., Bentley, K. T., and Schindler, D. E. 2015. Migration timing of adult Chinook salmon into the Togiak River, Alaska, watershed: Is there evidence for stock structure? *Transactions of the American Fisheries Society*, 144(4):829–836.
- de Valpine, P. and Hastings, A. 2002. Fitting population models incorporating process noise and observation error. *Ecological Monographs*, 72(1):57–76.
- Fleischman, S. J., Catalano, M. J., Clark, R. A., and Bernard, D. R. 2013. An age-structured state-space stock-recruit model for Pacific salmon (*Oncorhynchus* spp.). *Canadian Journal of Fisheries and Aquatic Sciences*, 70(3):401–414.
- Hamazaki, T. 2008. “When people argue about fish, the fish disappear.” Fishery closure “windows” scheduling as a means of changing the Chinook salmon subsistence fishery pattern: is it an effective tool? *Fisheries*, 33(10):495–501.
- Hamazaki, T. 2011. Reconstruction of subsistence salmon harvests in the Kuskokwim Area, 1990 – 2009. Fishery Manuscript Series 11-09, Alaska Department of Fish and Game, Anchorage, AK.
- Head, J. and Liller, Z. W. 2017. Salmon escapement monitoring in the Kuskokwim Area, 2016. Fishery Data Series 17-29, Alaska Department of Fish and Game, Anchorage, AK.
- Hendry, A. P. and Quinn, T. P. 1997. Variation in adult life history and morphology among Lake Washington sockeye salmon (*Oncorhynchus nerka*) populations in relation to habitat features and ancestral affinities. *Canadian Journal of Fisheries and Aquatic Sciences*, 54(1):75–84.

- Kellner, K. 2017. *jagsUI: A Wrapper Around 'rjags' to Streamline 'JAGS' Analyses*. R package version 1.4.9.
- Korman, J. and English, K. 2013. Benchmaark analysis for Pacific salmon conservation units in the Skeena watershed. A report to Pacific Salmon Foundation.
- Liller, Z. W., Hamazaki, H., Decossas, G., Bechtol, W., Catalano, M., and Smith, N. 2018. Kuskokwim River Chinook salmon run reconstruction model revision – executive summary. Regional Information Report 3A.18-04, Alaska Department of Fish and Game, Anchorage, AK.
- Ludwig, D. and Walters, C. J. 1981. Measurement errors and uncertainty in parameter estimates for stock and recruitment. *Canadian Journal of Fisheries and Aquatic Sciences*, 38(6):711–720.
- Newman, K. B., Buckland, S. T., Morgan, B. J. T., King, R., Borchers, D. L., Cole, D. J., Besbeas, P., Gimenez, O., and Thomas, L. 2014. *Modelling Population Dynamics*. Springer New York.
- Plummer, M. 2017. *JAGS Version 4.3.0 User Manual*.
- R Core Team 2018. *R: A Language and Environment for Statistical Computing*. R Foundation for Statistical Computing, Vienna, Austria.
- Raftery, A. E. and Lewis, S. 1992. How many iterations in the Gibbs sampler? In *Bayesian Statistics 4*, pages 763–773. Oxford University Press.
- Ricker, W. E. 1954. Stock and recruitment. *Journal of the Fisheries Research Board of Canada*, 11(5):559–623.
- Rose, K. A., Cowan, J. H., Winemiller, K. O., Myers, R. A., and Hilborn, R. 2001. Compensatory density dependence in fish populations: Importance, controversy, understanding and prognosis. *Fish and Fisheries*, 2(4):293–327.
- Schindler, D. E., Armstrong, J. B., and Reed, T. E. 2015. The portfolio concept in ecology and evolution. *Frontiers in Ecology and the Environment*, 13(5):257–263.
- Schindler, D. E., Hilborn, R., Chasco, B., Boatright, C. P., Quinn, T. P., Rogers, L. A., and Webster, M. S. 2010. Population diversity and the portfolio effect in an exploited species. *Nature*, 465(7298):609–612.
- Schnute, J. T. and Kronlund, A. R. 2002. Estimating salmon stock-recruitment relationships from catch and escapement data. *Canadian Journal of Fisheries and Aquatic Sciences*, 59(3):433–449.
- Shelden, C. A., Hamazaki, T., Horne-Brine, M., and Roczicka, G. 2016. Subsistence salmon harvests in the Kuskokwim Area, 2015. Fishery Data Series 16-55, Alaska Department of Fish and Game, Anchorage, AK.
- Smith, N. J. and Liller, Z. W. 2017a. Inriver abundance and migration characteristics of Kuskokwim River Chinook salmon, 2015. Fishery Data Series 17-22, Alaska Department of Fish and Game, Anchorage, AK.

- Smith, N. J. and Liller, Z. W. 2017b. Inriver abundance and migration characteristics of Kuskokwim River Chinook salmon, 2016. Fishery Data Series 17-47, Alaska Department of Fish and Game, Anchorage, AK.
- Staton, B. 2018a. *codaTools: Utilities for Dealing with mcmc.lists*. R package version 0.1.1 available at <https://github.com/bstaton1/codaTools>.
- Staton, B. 2018b. *FitSR: Functions to Fit and Summarize SRA Models*. R package version 0.1.2 available at <https://github.com/bstaton1/FitSR>.
- Staton, B. 2018c. *SimSR: Tools for Simulating Pacific Salmon Spawner-Recruit Dynamics*. R package version 0.1.2 available at <https://github.com/bstaton1/SimSR>.
- Staton, B. A., Catalano, M. J., and Fleischman, S. J. 2017. From sequential to integrated bayesian analyses: Exploring the continuum with a pacific salmon spawner-recruit model. *Fisheries Research*, 186:237–247.
- Su, Z. and Peterman, R. M. 2012. Performance of a Bayesian state-space model of semelparous species for stock-recruitment data subject to measurement error. *Ecological Modelling*, 224(1):76–89.
- Templin, W. D., Smith, C. T., and D. Molyneaux, L. W. S. 2014. Genetic diversity of Chinook salmon from the Kuskokwim River. USFWS Office of Subsistence Management, Fisheries Resource Monitoring Program, Final Report 01-070, Alaska Department of Fish and Game, Anchorage, AK.
- Walters, C., English, K., Korman, J., and Hilborn, R. 2018. The managed decline of British Columbia's commercial salmon fishery. *Marine Policy*. Pre-print as of 2/18/2019; DOI: 10.1016/j.marpol.2018.12.014.
- Walters, C. J. 1985. Bias in the estimation of functional relationships from time series data. *Canadian Journal of Fisheries and Aquatic Sciences*, 42(1):147–149.
- Walters, C. J., Lichatowich, J. A., Peterman, R. M., and Reynolds, J. D. 2008. Report of the Skeena independent science review panel. A report to the Canadian Department of Fisheries and Oceans and the British Columbia Ministry of the Environment.
- Walters, C. J. and Martell, S. J. D. 2004. *Fisheries Ecology and Management*. Princeton University Press.